WILEY-BLACKWELL

Cladistics 34 (2018) 652–683

Cladistics

10.1111/cla.12227

Total evidence analysis and body size evolution of extant and extinct tortoises (Testudines: Cryptodira: Pan-Testudinidae)

Evangelos Vlachos[a,b,*] and Márton Rabi[c,d]

[a]*CONICET – Museo Paleontológico Egidio Feruglio, Av. Fontana 140, Trelew, Chubut, 9100 Argentina;* [b]*School of Geology, Aristotle University of Thessaloniki, Thessaloniki, Greece;* [c]*Central Natural Science Collections, Martin-Luther University Halle-Wittenberg, Domplatz 4, 06108 Halle (Saale), Germany;* [d]*Department of Geosciences, University of Tübingen, Hölderlinstrasse 12, 72074 Tübingen, Germany*

Accepted 18 September 2017

Abstract

Testudinidae (tortoises) is an extant clade of terrestrial turtles of worldwide distribution and with a rich fossil record that provides an exceptional context for studying their evolutionary history. Because of the lack of global phylogenetic analyses integrating extinct taxa, our current knowledge of the relationships of the total clade of Testudinidae is rather poor. To resolve this issue, we performed the first total evidence analysis of Pan-Testudinidae. The total evidence trees are congruent with the molecular topology and agree on the dichotomy of derived Testudinidae (=Testudininae; Converted Clade Name) into two previously recognized major clades, Testudona and Geochelona (New Clade Name). The integration of extinct taxa into the analysis allowed the stratigraphic fit of the total evidence trees, indicating that crown Testudininae, Testudona and Geochelona all originated by the Late Eocene, in agreement with recent molecular estimates. Ghost lineage analysis indicates high diversification in the Late Eocene and in the Miocene. The age of crown *Testudo* is Late Miocene, again in accordance with some molecular dates. Phylogenetic placement of fossils demonstrates that giant body size independently evolved in multiple continental mainland taxa and confirms recent results deduced from living taxa—giantism in Testudinidae is not linked to the insular effect. An unexpected outcome is the recovery of miniaturization in Testudona (<30 cm carapace length) that emerged sometime between the Oligocene and Early Miocene. No clear correlation between body size evolution and climate is apparent, but increased taxon sampling may nevertheless demonstrate the role of cooling and warming as one of many influential variables.

Introduction

Testudinidae is an extant clade of terrestrial turtles (tortoises) comprising at least 43 extant species (see Joyce et al., 2004; appendix 8). Testudinids are globally distributed on all continents except Australia and Antarctica and are adapted to diverse terrestrial environments ranging from arid deserts, to humid forests, as well as isolated insular environments (Ernst and Barbour, 1989; Swingland and Klemens, 1989). Some species evolved large sizes that can exceed 1 m in carapacial length and, as such, have received particular interest from naturalists ever since the times of Darwin (e.g., the Galápagos tortoises).

Members of this clade were among the first turtles to be named and studied since the times of Linnaeus (1758) with the description of the iconic taxon name *Testudo*. Thus, this group of turtles has an extensive literature and a vast and complex nomenclatural history. The recognition of tortoises (=Testudinidae) as a natural group has never been seriously questioned and the monophyly of this clade has been strongly supported both by molecular (Le et al., 2006; Fritz and Bininda-Emonds, 2007; Guillon et al., 2012) and morphological data (Auffenberg, 1974; Crumly, 1984; Gaffney and Meylan, 1988; Joyce and Bell, 2004).

Revision of the taxonomy of fossil Pan-Testudinidae is due and, as such, it is difficult to estimate the number of valid extinct species. Auffenberg (1974) lists more than 200 extinct species, Bramble and Hutchison (2014) and Franz (2014) list more than 30 species for

*Corresponding author.
E-mail address: evlacho@mef.org.ar

North America alone, and Lapparent de Broin (2001) records at least seven genera of tortoises with more than 30 species combined for Europe.

Numerous previous works have attempted to reconstruct phylogenetic relationships within testudinids although sampling of fossil taxa and morphological data have been limited. Crumly (1982, 1984) was the first to apply cladistic methodology to tortoises using skeletal and soft tissue data. Gerlach (2001) defined a new set of cranial characters and expanded taxon sampling. Meylan and Sterrer (2000; expanded by Takahashi et al., 2003) added few extinct taxa (e.g., *Stylemys*, *Hesperotestudo*) to a matrix comprising mainly extant species. Perälä (2002) presented a morphological phylogeny of the *Testudo* clade. Several molecular works provided further resolution within extant Testudinidae (Le et al., 2006; Fritz and Bininda-Emonds, 2007; Guillon et al., 2012).

Three main clades have been distinguished with consensus in molecular studies: (i) a basal clade of *Manouria* + *Gopherus* spp., (ii) the clade Testudona Parham (in Parham et al., 2006) containing small taxa (*Testudo*, *Indotestudo*, *Malacochersus* spp.), and (iii) a diverse clade referred to as the "*Geochelone* complex" (Parham et al., 2006), containing African, Asian and South American taxa (species of *Aldabrachelys*, *Pyxis*, *Stigmochelys*, *Psammobates*, *Geochelone*, *Centrochelys*, *Kinixys* and *Chelonoidis*). This topology is generally strongly supported by molecular data with a few exceptions (e.g., the sister-group relationship of *Manouria* and *Gopherus*; the sister-group relationships of *Malacochersus* and *Indotestudo*; the derived position of *Kinixys* within the "*Geochelone* complex"). Other molecular studies focused on more exclusive clades including *Gopherus* spp. (Lamb and Lydeard, 1994), Testudona (Parham et al., 2006) and *Kinixys* spp. (Kindler et al., 2012). Recently, Lapparent de Broin et al. (2006; expanded by Corsini et al., 2014 and Luján et al., 2016) explored the relationships within forms usually considered as close relatives of *Testudo* (a classic "waste-basket" taxon of Testudinidae) including numerous extinct, circum Mediterranean testudinid taxa. Luján et al. (2014) added the extinct taxon *Cheirogaster* to the matrix of Gerlach (2001). Pérez-García and Vlachos (2014) analysed a small matrix of extinct testudinid taxa and proposed that *Cheirogaster* (another "waste-basket" taxon for Europe) is restricted to the type species *Cheirogaster maurini* and therefore European Neogene large testudinids form a distinct clade. Building upon this matrix, Pérez-García (2016) and Pérez-García et al. (2016) have added more extinct taxa and characters exploring the phylogenetic relationships of Palaeogene pan-testudinids in further detail. Vlachos (2015), in his doctoral thesis, and later Vlachos and Tsoukala (2016) presented a new matrix with an expanded sample of European fossil testudinids that served as the basis for the matrix presented herein.

The main goal of the current study is to increase phylogenetic resolution for extinct testudinids based on a combined analysis of morphological and molecular data. Our main focus is on European (i.e., western Palearctic) tortoises, but our analysis helps to establish broader conclusions at a global scale. A total evidence analysis is performed for the first time for Testudinidae (an approach that has been used for other clades of Testudinata; e.g., Burke et al., 1996; Shaffer et al., 1997; Lee, 2001; Sterli, 2010). The key questions we aim to answer are the following:

1. Are extinct small Palearctic testudinids closely related to *Testudo*? Extant tortoises from the Mediterranean region indeed form part of the monophyletic Pan-*Testudo* clade (*sensu* Parham et al., 2006) but the rich Cenozoic fossil record of Europe is yet to be integrated into a global phylogenetic context.
2. Do large Palearctic testudinids form a monophyletic group? Until recently, most large Palearctic tortoises have been included in the genus *Cheirogaster*. A new generic name, *Titanochelon*, has been proposed for the Neogene giant forms (Pérez-García and Vlachos, 2014) but the monophyly and relationships of large-sized taxa remains untested in a global phylogeny.
3. Is small body size of extant testudinids a derived or ancestral trait and did giantism evolve once or several times in tortoises? Body size evolution has not been previously analysed through a species-level global phylogeny of pan-testudinids.

Material and methods

Character sampling

We expanded the species-level Testudinoidea morphological matrix of Joyce and Bell (2004) – 53 taxa × 70 characters; Fig. 1). While we acknowledge that their matrix is not designed to resolve interrelationships within Testudinidae, our decision to build on this matrix was for following reasons: (i) it presents a detailed overall review of morphological characters; (ii) ontogenetic variation and sexual dimorphism are evaluated and taken into account in character design; and (iii) testudinid outgroup taxa are extensively sampled. Character sampling was expanded by the critical review of previously used morphological studies on Testudinidae and Testudinoidea (e.g., Crumly, 1984 – 39 taxa × 54 characters; Gerlach, 2001 – 24 taxa × 60 characters; Claude and Tong, 2004 – 20 taxa × 44 characters; Lapparent de Broin et al., 2006 – 23 taxa

× 18 characters; Pérez-García and Vlachos, 2014 – 9 taxa × 36 characters) and by the addition of new characters (Fig. 1; see Appendix for character list and definitions). Some characters were taken or modified from Hirayama (1985), Gaffney and Meylan (1988), Meylan and Sterrer (2000), Perälä (2002) and Hervet (2003). We attempted to include clearly reproducible characters only, while we acknowledge that some omitted characters could be potentially useful and should be reviewed in the future (see Appendix).

Character states

We have reviewed all multistate characters in order to argue in favour of reductive or composite coding and on the necessity of ordering characters. Following Wilkinson (1995), a reductive coding (i.e., "breaking" a composite character into binary characters) was preferred when the complex of variation is biologically independent to avoid overweighting variation. On the other hand, in cases where the observed variation could be biologically dependent, a composite (i.e., multistate) character was constructed. Multistate characters forming a morphocline were treated as ordered.

Taxon sampling

The taxon sample of Joyce and Bell (2004) was expanded through direct study of skeletal material of the following taxa: *Manouria impressa*, *Kinixys erosa*, *Astrochelys radiata*, *Chelonoidis carbonaria*, *Chelonoidis denticulata*, *Chelonoidis chilensis*, *Centrochelys sulcata*, *Geochelone elegans*, *Indotestudo forstenii*, *Testudo kleinmanni*, *Chersine hermanni* and *Testudo marginata*. Four more extant and 36 extinct testudinids were added (Fig. 1 and Appendix for detailed information). The majority of emydid and geomeydid taxa from the matrix of Joyce and Bell (2004) have been omitted as those are

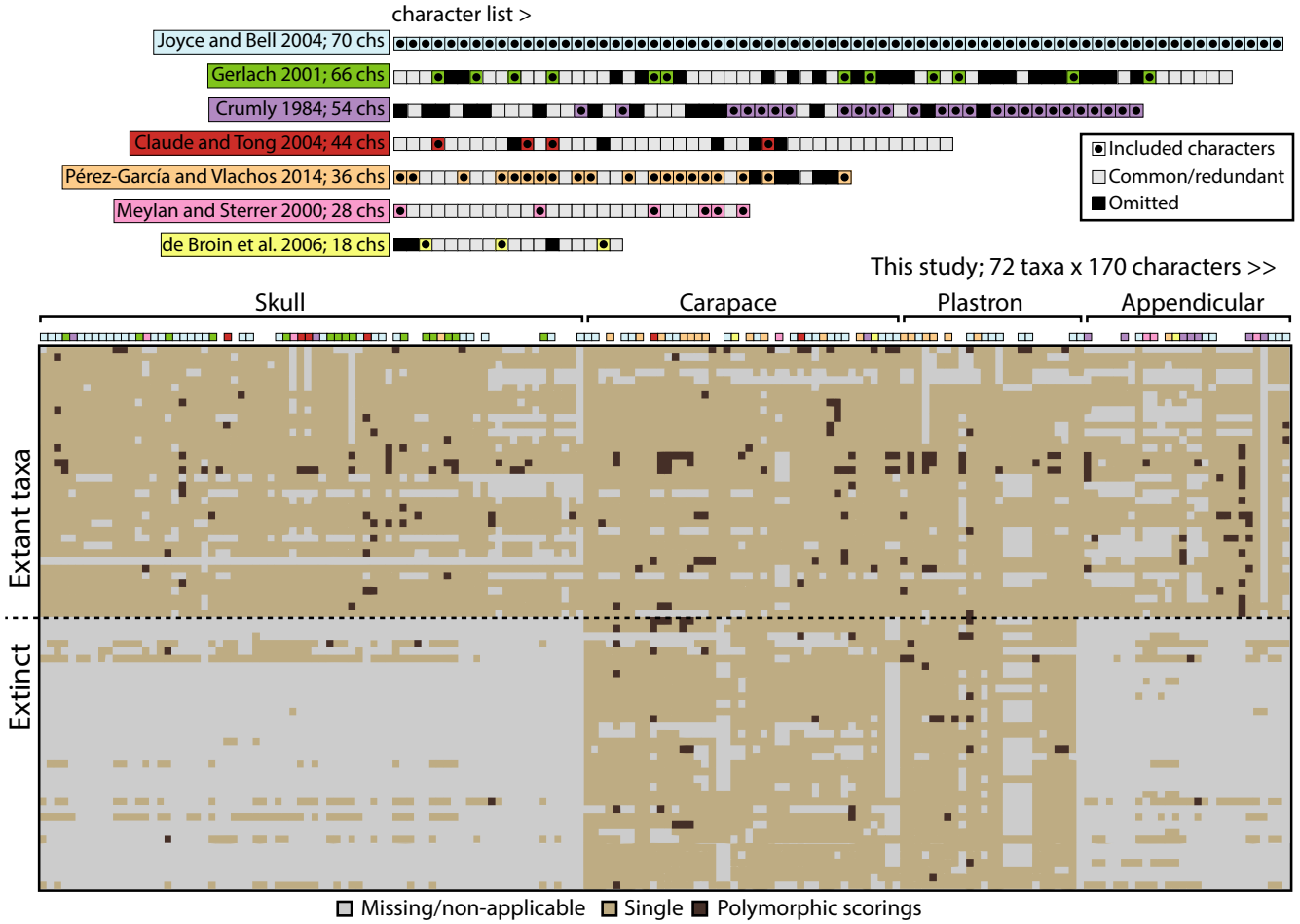

Fig. 1. Composition of the morphological character matrix relative to previous studies. Characters with a solid circle are included in the matrix, characters in grey are redundant and/or common among the matrices, whereas characters in black are omitted (see Appendix for more information). The matrix of the current study contains the entire character list of Joyce and Bell (2004; light blue), a selection of characters from other published matrices and some new characters. Most of the missing information is found in the skull and appendicular elements of extinct taxa. [Color figure can be viewed at wileyonlinelibrary.com]

not the focus of the present work. Additional outgroups include selected representatives of each major cryptodire "family" and a composite pleurodire clade.

Morphological matrix

Our final morphological matrix contains 72 taxa and 170 characters (Fig. 1 and Appendix; Supporting Information, File S1 for NEXUS format). In total, 37.23% of the matrix contains missing entries, mostly in the extinct taxa (Fig. 1). Most of these missing entries are from the skull and appendicular skeleton (Fig. 1). Non-applicable entries and polymorphic scorings represent a negligible part of the matrix (0.02% in each case).

Molecular matrix

For analysis of the molecular data we used the composite aligned global turtle matrix of Guillon et al. (2012) available for download in treebase.org [20 000 characters from five mitochondrial (12S, 16S, COI, NAD4, cytB) and four nuclear genes (R35, c-mos, RAG1, RAG2). Taxon sampling was reduced to the extant taxon sampling of our morphological analysis (Appendix). Parsimony analysis of this reduced data set (traditional search TBR algorithm in TNT; Goloboff et al., 2008) recovered a consistent topology with that of Guillon et al. (2012).

Analyses and software

The matrix was analysed with extant taxa only (Fig. 2), as well as with the addition of extinct taxa (Fig. 3). For each taxon sample, two parsimony analyses were performed, one using morphological characters alone and another using both morphological and molecular data (total evidence). The morphological data were analysed using a traditional search TBR algorithm in TNT (Goloboff et al., 2008) with 1000 replicates. Where necessary, a second traditional search (TBR) with all trees from RAM was performed to obtain all most parsimonious trees (MPTs). The total evidence matrix was analysed using a New Technology Search (NTS) in TNT combining all search options (sectorial, tree-drifting, tree-fusing, ratchet) with the aim to hit the shortest tree at least 27 times. A second traditional search (TBR) with all trees from RAM was performed to obtain all MPTs. After the MPTs were obtained, another NTS was performed aiming to find even shorter trees, to ensure that the most parsimonious solution was obtained. All synapomorphies discussed in the text are unambiguous and common in all trees unless otherwise stated. All synapomorphies are listed in Files S2 and S4. Bootstrap and jackknife supports (GC, Group Present/Contradicted; Goloboff et al., 2003) were calculated with the Resampling command in TNT and Bremer supports were calculated with the bremer.run script (shown in Figs 2–4). Consistency and retention indices (CI, RI) were calculated with the wstats.run script. For the analysis of unstable taxa we used Pruned Trees in TNT and the IterPCR script of Pol and Escapa (2009) (File S3). Morphological MPTs of extant taxa were placed in a single .ctf file together with molecular MPTs. The IterPCR script identified wildcard taxa and the characters responsible for the different position in the two topologies. The modified Manhattan stratigraphic measure (MSM*) and the script MSM.run in TNT were used for time calibration of the total evidence consensus tree (Pol and Norell, 2001). Patterns of diversification were calculated by raw counts of taxa (taxic diversity) and raw counts of lineages (phylogenetic diversity) per stage (see Norell, 1992; Pol and Leardi, 2015; and references therein).

Body size analysis

Midline carapacial length data of extant and extinct taxa were collected from the literature (Ernst and Barbour, 1989; and references therein) and through direct measurements of specimens (File S5). A separate matrix was created with a single continuous character of carapace length and was subsequently mapped and optimized on the MPTs of the total evidence analysis (following Gould and MacFadden, 2004; and references therein). Size evolution was reconstructed for the total evidence tree by estimating the plesiomorphic body size for each clade based on the results of character mapping in TNT. Statistical and regression analyses were performed with a LOESS model in PaSt v.3 (Hammer et al., 2009) to assess significance. To test the sensitivity of the results to topological changes, the same procedure was repeated on a total evidence topology retrieved from an analysis using implied character weighting (Mirande, 2009; Mirande et al., 2013; Goloboff, 2014). The trees from the implied weight (IW) analysis are compared to those of the equally weighted (EW) total evidence analysis (using standard measures such as Robinson–Foulds distances, distortion coefficient and Subtree Prune and Regraft' distances, implemented in TNT; File S8). The selected trees from the IW analysis were used to map and analyse body size as described above (File S8).

All these files, as well as other accompanying files, are stored and available as Project 2627 of Morphobank (http://morphobank.org/permalink/?P2627).

Results

Analyses of extant taxa

Analysis of the morphological matrix of the extant taxa resulted in two MPTs (Fig. 2A; TBR; best score

536 out of 1000; CI: 0.323; RI: 0.642) of 609 steps. As far as the outgroups are concerned, Emydidae is not recovered as a monophyletic group and *Platysternon* is recovered as sister to *Apalone*. The relationships within Testudinidae show some further differences compared to molecular phylogenies (Le et al., 2006; Fritz and Bininda-Emonds, 2007; Guillon et al., 2012): *Manouria* is not monophyletic, *Kinixys* with *Malacochersus* are placed in a basal position and relationships within the "*Geochelone* complex" are not fully resolved. Strongly supported clades (bootstrap GC: jackknife GC: Bremer) within Testudinidae include *Kinixys* spp. (94:99:8), *Gopherus* spp. (97:98:8), *Chelonoidis carbonaria* + *Chelonoidis denticulata* (85:90:4) and *Testudo marginata* + *Testudo graeca* (38:54:3; Fig. 2A). As it is evident from the GC frequencies (bootstrap and jacknife of group present/contradicted values; Goloboff et al., 2003), there is a great deal of character conflict among most testudinid clades. The monophyly of Testudinidae is nevertheless strongly supported by 15 synapomorphies (see File S2), most of which are classic testudinid synapomorphies (e.g., closure of insicura columella auris; wide fissure ethmoidalis; descending processes of the frontals; wide and expanded coracoid; no webbing between the digits; phalangeal reduction).

The total evidence analysis of the extant taxa resulted in two MPTs (Fig. 2B; TBR; best score 1000 out of 1000; CI: 0.495; RI: 0.458) of 17 902 steps. Support is relatively strong for all clades, yet some (e.g., within the "*Geochelone*" complex) still show some character conflict (lower GC frequencies in Fig. 2B). Again, the morphological support for the clade Testudinidae is strong with 20 synapomorphies [see File S2; e.g., additional to those mentioned above: coincidence between pleuromarginal sulci and costo-peripheral sutures; fused trochanters of the femur; ridge on the vomer; shape of the suprapygals (Appendix, Fig. 17)]. Node Testudininae (i.e., Testudona + "*Geochelone* complex") is also strongly supported by seven synapomorphies (see File S2; e.g., foramen carotico-pharyngeale absent; interdigitated suture between surangular and dentary; long major trochanter of the humerus; radius completely separated from the distal carpals). Clade Testudona is supported by four synapomorphies [see File S2; long and elongated prootic; foramen jugulare posterius in exoccipital/opisthotic suture; coronoid excluded from foramen alveolare posterius; pleural 1 touches but does not overlap the lateral sides of the nuchal (Appendix, Fig. 16)]. The node of the "*Geochelone* complex" is supported only by one synapomorphy (see File S2; medial tooth present in the dentary) but the clades within this complex are more strongly supported (see File S2). Another character that supports the two main clades of Testudininae is the absence/presence of a contact between marginal 6 and pleural 3 (absent in Testudona; present in the "*Geochelone* complex"), but is not recovered as a synapomorphy for any of these clades due to the ambiguous optimization (see the mapping of this character in Fig. 2B).

Character conflict and unstable taxa

To analyse the differences between the morphological and the molecular/total evidence topologies, an analysis with the iterPCR script (Pol and Escapa, 2009) was performed (see Methods) on a set of trees combining the morphological and molecular topologies recovered above. The script identifies the taxa in different positions in the morphological and molecular topology as "unstable taxa" and determines the characters that are responsible for this conflict. The results are given in Supporting Information, File S3. The script identified a number of outgroup and testudinid taxa that have conflicting positions in the morphological and molecular topologies. The testudinids include *Kinixys* spp., *Malacochersus tornieri*, *Testudo kleinmanni*, *Astrochelys radiata*, *Psammobates oculifera*, *Chelonoidis denticulata* and *Chel. carbonaria*. As far as the outgroups are concerned, we can conclude that a significant number of characters from the entire skeleton support alternative positions in the trees. This is not surprising as the character sample in our matrix was designed with a clear testudinoid (and especially testudinid) focus. The greatest conflict for the ingroup is caused by two highly specialized taxa, *Kinixys* and *Malacochersus*. They form a clade in a basal position in the morphological tree, but are pulled in a more derived position in the molecular tree (*Malacochersus* basal within Testudona; *Kinixys* derived within the "*Geochelone* complex"). The morphological topology is supported by 11 synapomorphies but has a low Bremer support and low GC frequencies. Although at a first look the support of this clade seems strong, the results of the script explain the unexpected grouping and basal position of *Kinixys* and *Malacochersus* in the morphological phylogeny (File S3). First, many characters are scored as not applicable for *Malacochersus* due to the heavily reduced bony shell of this species. Indeed, the script identifies those missing characters (mainly from the carapace) for *Malacochersus* as potentially important for resolving the position of this taxon. At the same time, these missing carapacial characters in *Malacochersus* are identified as partly responsible for placing *Kinixys* in this basal position. *Kinixys* is also specialized in having a carapacial hinge, which may be responsible for the reorganization of plate and scute configuration in the carapace. Also, although in molecular analyses *Kinixys* is always recovered in a derived position, its skull morphology shows several traits that are plesiomorphic for Testudinidae [e.g., the absence of

serration and tooth-like tubercles; reduced upper temporal emargination (Appendix, Fig. 8), absence of additional ridges in the palate (Appendix, Fig. 9), short vomer (Appendix, Fig. 11)], which place this clade in a more basal position in the morphological analysis. Most of these characters are returned as conflicting by the script. As such, this unusual grouping could be explained by the highly specialized morphology of these tortoises: as the conflicting shell characters in *Kinixys* cannot be scored in *Malacochersus*, a secondary set of synapomorphies draws the two taxa together, and primarily the cranial characters of *Kinixys* place this unexpected clade in a basal position within Testudinidae. Curiously, the placement of these taxa has low support in molecular analyses as well (Le et al., 2006; Fritz and Bininda-Emonds, 2007; Guillon et al., 2012). Mautner et al. (2017) recently revised the anatomy of *Malacochersus*, demonstrating not only the specializations of the shell but also a high degree of variability of the bones and scutes of the carapace and plastron. Our results highlight that in-depth analysis of character conflict can provide useful insights into the contrast between morphological and molecular topologies.

Homoplasy

Homoplasy within Testudinidae has been already pointed out by Auffenberg (1974) and has been reported in nearly all published phylogenies of testudinids. We further analysed the homoplasy per character group (i.e., cranial, shell and appendicular skeleton) for the morphological matrix on the final topology of the complete total evidence analysis. From the three different character groups, shell characters are the most homoplastic (CI = 0.188–0.189), followed by cranial characters (CI = 0.259–0.260). Appendicular characters are the least homoplastic (CI = 0.354). In all cases, the RI is considerably higher than CI (cranial = 0.610; shell = 0.557; appendicular = 0.654).

Phylogenetic taxonomy of Pan-Testudinidae

We provide definitions for some new (NCN) and converted clade names (CCN) that will help the communication of palaeontologists and neontologists working with Pan-Testudinidae. In particular, we provide a CCN for the well-supported clade that unites the "*Testudo* complex" and the "*Geochelone* complex" and an NCN for the "*Geochelone* complex".

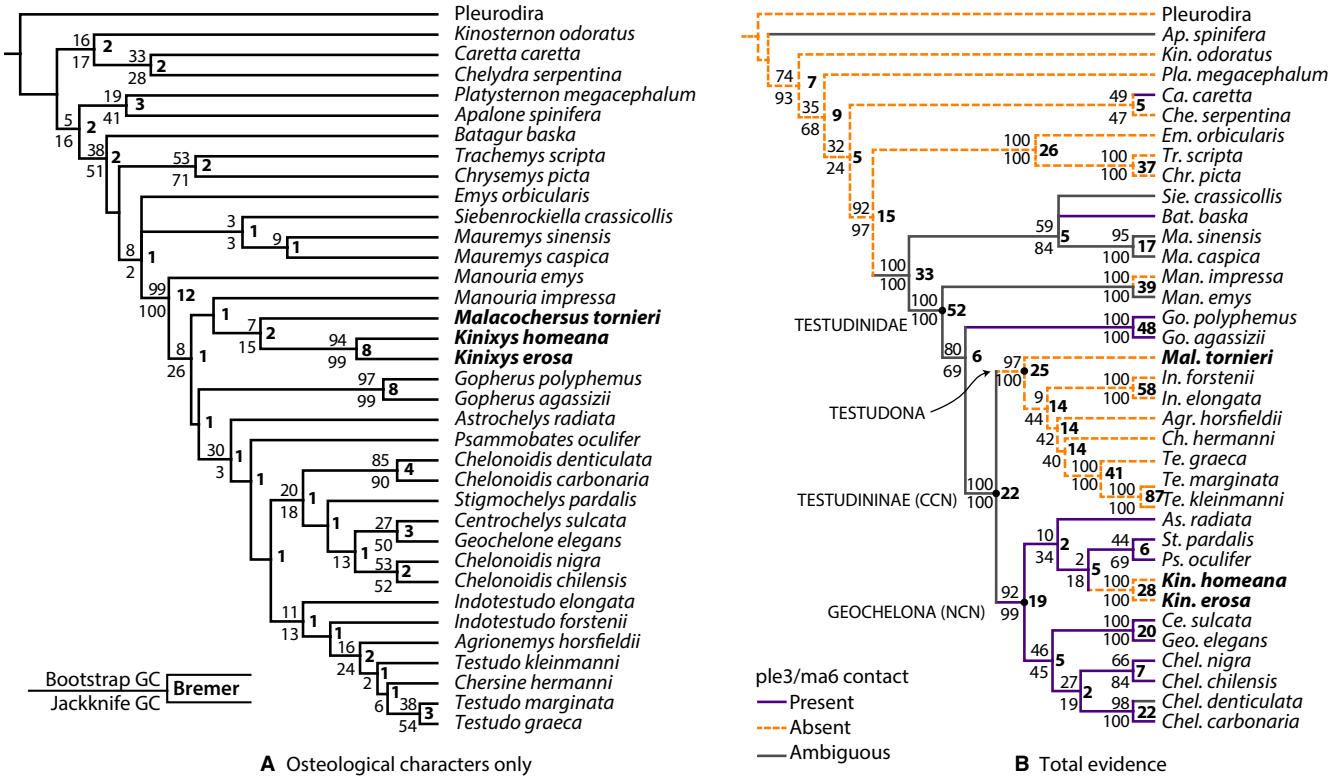

Fig. 2. A, strict consensus of the most parsimonious trees of extant taxa, using osteological characters. B, total evidence analysis of extant taxa. *Malacochersus tornieri* and *Kinixys* spp. (in bold) are primarily responsible for the topological differences (see text for more details). Coloured branches in B denote the optimization of the contact between pleural 3 and marginal 6 (see text for details). [Color figure can be viewed at wileyonlinelibrary.com]

Testudininae Batch, 1788 (CCN). This name refers to the crown clade originating from the last common ancestor of *Geochelone elegans* (Schoepff, 1795) and *Testudo graeca* Linnaeus, 1758. Members of Testudininae are characterized by the following combination of characters: no foramen caroticopharyngeale, strongly interdigitated suture between the surangular and the dentary, cervical scute longer than wide (lost subsequently within Testudininae), long major trochanter of the humerus, no contact between the radius and the distal carpals.

Geochelona (NCN). This name refers to the clade that has been given the informal name "*Geochelone* complex" by Parham et al. (2006). Molecular support is strong for this clade based on recently published analyses (Le et al., 2006 = 100; Fritz and Bininda-Emonds, 2007 = 94.8–99.1–100; Guillon et al., 2012 = 1.000). As a result of inconsistent use of the name "*Geochelone*" for polyphyletic and paraphyletic groups (by both neontologists and palaeontologists), the communication of this clade has been problematic. As such the use of any pre-existing family-group names stemming from *Geochelone* would be misleading. We hope that the definition of this new clade name will improve this situation.

We formally propose the new name (NCN) Geochelona for this clade, by using the stem of genus *Geochelone* Fitzinger, 1826. The name draws a clear parallel to its sister clade Testudona Parham (in Parham et al., 2006). The node-based definition of this clade is as follows: the clade Geochelona (NCN) is defined as the crown clade originating from the last common ancestor of *Psammobates* (*Stigmochelys*) *pardalis* (Bell, 1828), *Chelonoidis chilensis* (Gray, 1870), *Geochelone elegans* (Schoepff, 1795), *Astrochelys radiata* (Shaw, 1802). The members of Geochelona[1] are characterized by the following combination of characters: frontals longer than prefrontals (Appendix, Fig. 6); presence of a foramen nervi auriculotemporalis (subsequently lost in *Kinixys*); medial tooth present in the dentary; interdigitated suture between surangular and dentary; long major trochanter of the humerus that extends beyond the head of the humerus; radius completely separated by the distal carpals; contact of the sixth marginal with the third pleural scute (subsequently lost in *Kinixys*). Pre-existing family-group names include the tribe name Geochelonini Crumly (in Swingland and Klemens, 1989), with a polyphyletic composition with respect to the clade named herein.[2]

Analyses with extinct taxa included

The first run of the complete morphological matrix including all extinct taxa resulted in 10 MPTs (TBR; best score 4 out of 1000; overflow) of 845 steps. Due to the low number of hits, we made a second run that resulted in 33 MPTs (New Technology; best score hit 27 times) of 845 steps. The final run with the trees from RAM resulted in 40 MPTs of 845 steps (Fig. 3A; CI: 0.243; RI: 0.612). The inclusion of fossils in the analysis resulted in much lower support for all clades and a larger amount of character conflict. The total evidence analysis produced 50 MPTs of 18 142 steps (Figs 3B and 4; NTS; best score hit 27 times; CI: 0.489; RI: 0.460). The following discussion on the position and phylogenetic relationships of the extinct taxa is based on the results of the total evidence analysis (Figs 1 and S3). The full list of synapomorphies is given in Supporting Information, File S4. Below, we thoroughly discuss and evaluate the robustness of our results and the placement of extinct taxa based on the support values and synapomorphies of each group, as well as external evidence when available.

Non-pan-testudinids. The only extinct taxon recovered outside Pan-Testudinidae is *Anhuichelys siaoshihensis* Yeh, 1979, as a member of Emydidae and a sister-group of the *Trachemys* + *Chrysemys* clade

[1]Living species of Geochelona (generic combinations mostly follow Fritz and Bininda-Emonds, 2007): *Chersina angulata* (Schweigger, 1812); *Dipsochelys dussumieri* (Gray, 1831); *Chelonoidis carbonaria* (Spix, 1824); *Chelonoidis chilensis* (Gray, 1870); *Chelonoidis nigra* (Quoy and Gaimard, 1824); *Chelonoidis denticulata* (Linnaeus, 1766); *Geochelone elegans* (Schoepff, 1795); *Geochelone platynota* (Blyth, 1863); *Stigmochelys pardalis* (Bell, 1828); *Astrochelys radiata* (Shaw, 1802); *Astrochelys yniphora* (Vaillant, 1885); *Centrochelys sulcata* (Miller, 1779); *Homopus areolatus* (Thunberg, 1787); *Homopus boulengeri* Duerden, 1906; *Homopus femoralis* Boulenger, 1888; *Homopus signatus* (Schoepff, 1801); *Kinixys belliana* Gray, 1831; *Kinixys erosa* (Schweigger, 1812); *Kinixys homeana* Bell, 1827; *Kinixys lobatsiana* Power, 1927; *Kinixys natalensis* Hewitt, 1935; *Kinixys spekii* Gray, 1863; *Malacochersus tornieri* (Siebenrock, 1903); *Psammobates oculifer* (Kuhl, 1820); *Psammobates tentorius* (Bell, 1828); *Pyxis arachnoides* Bell, 1827; *Pyxis planicauda* (Grandidier, 1867).

[2]In Swingland and Klemmens (1989), the classification of Testudinidae is based mainly on Crumly (1984). Therein, tribe Geochelonini contains the following taxa: *Geochelone elephantopus* or *nigra*, *G. denticulata*, *G. carbonaria*, *G. chilensis*, *G. elegans*, *G. platynota*, *G. gigantea*, *G. radiata*, *G. yniphora*, *G. pardalis* and *G. sulcata*. The tribe Testudinini is defined therein as containing the following species: *Acinixys planicauda*, *Homopus areolatus*, *H. bergeri*, *H. boulengeri*, *H. femoralis*, *H. signatus*, *Indotestudo elongata*, *I. forstenii*, *Malacochersus tornieri*, *Psammobates geometricus*, *P. oculifer*, *P. tentorius*, *Pyxis arachnoides*, *Testudo marginata*, *T. graeca*, *T. hermanni*, *T. horsfieldii*, *T. kleinmanni*, *Kinixys belliana*, *K. erosa*, *K. homeana* and *K. natalensis*. In their classification, the subfamily Geochelonine contains both tribes mentioned above. Hutterer et al. (1997) furthermore lists the extinct taxa *Geochelone burchardi* (Ahl, 1927), *Geochelone vulcanica* (López-Jurado and Mateo, 1993) and two unnamed species from the Canary Islands as members of Geochelonini.

(Figs 3B and 4). Its grouping with Emydidae is supported by three synapomorphies (humerals equal to or smaller than gulars; no anal notch; pygal configuration), whereas the absence of axillary glands groups it with the *Trachemys* + *Chrysemys* clade. Besides the above-mentioned synapomorphies, several characters (rectangular neural 1; hexagonal neural 2 with short sides positioned anteriorly) exclude this taxon from the stem of Pan-Testudinidae. This taxon was recently revised by Tong et al. (2016; on which our scorings are based). In most of their analyses, they recover *Anhuichelys* as the sister taxon of Testudinidae but without strong support (Tong et al., 2016: 175). They nevertheless consider it likely that *Anhuichelys* is the oldest Testudinidae because of the presence of alternating costals 2–6 (although, corresponding alternating neurals are absent). The position of *Anhuichelys* nested within Emydidae recovered herein is inconsistent with its stratigraphic distribution and would imply a complex biogeographical history. We therefore emphasize that the affinities of this taxon should be further investigated, although it is probably not a pan-testudinid.

Stem testudinids. The clade Pan-Testudinidae is supported by five synapomorphies (hexagonal neural 1 with short sides positioned posteriorly; rectangular neural 2; narrow and thin rib heads (Appendix, Fig. 18); absence of axillary glands; fused trochanters of the femur), suggesting several important morphological changes in the shell compared to emydids and geoemydids. "*Achilemys*" *cassouleti* Claude and Tong, 2004 from the Early Eocene of France is recovered as the basal-most taxon in the stem, supporting the suggestion of Claude and Tong (2004: 19) that it represents the most basal member of Testudinidae (= Pan-Testudinidae herein). This position is due to the distinct pattern of the first four neurals (6P<4 < 8<4), the straight contact of the two suprapygals (Appendix, Fig. 17), the absence of gular protrusion, the gulars not reaching the entoplastron, the wide gularo-humeral sulcus, and the perpendicular humero-pectoral sulcus. The type species of *Achilemys* is *Achilemys allabiata* (Cope, 1872) from the Bridgerian of Wyoming, USA (see Hay, 1908). Recently, Pérez-García and Vlachos (2014) and Pérez-García (2016) questioned the attribution of the Saint Papoul taxon to *Achilemys*. Finally, Pérez-García et al. (2016) performed a new analysis including both *cassouleti* and *allabiata*, failing to recover them in the same clade. Given the many morphological differences between the two taxa, they erected the new genus *Fontainechelon* for "*Achilemys*" *cassouleti*. Our analysis shows that the morphological information of the type material of *Ach. allabiata* is very limited, not allowing a clear diagnosis beyond the level of Pan-Testudinoidea and as such *Ach. allabiata* can be considered a nomen dubium. Furthermore, our analysis failed to associate "*Ach.*" *cassouleti* with any other named genus or clade, and as such the new generic name *Fontainechelon* seems appropriate for the moment. *Fontainechelon* is the basalmost pan-testudinid to our knowledge, but not the oldest one. *Hadrianus majusculus* Hay, 1904 from the Ypresian of North America is currently considered the oldest pan-testudinid (see Joyce et al., 2013). Because of the lack of carapacial information for this taxon, we omitted it from our analysis. The morphology of *Hadrianus majusculus* is slightly more derived than *Fontainechelon* (e.g., narrower and longer gular scutes; "wavy" humero-pectoral sulcus with medial part being convex anteriorly). *Hadrianus majusculus* is certainly a pan-testudinid and pushes the origin of the group at least to the Palaeocene, in accordance with recently published molecular clocks (Lourenço et al., 2012; Joyce et al., 2013).

In a slightly more derived position compared to *Fontainechelon*, we recover the recently named *Pelorochelon soriana* Pérez-García et al., 2016 from the Bartonian of Spain. *Pelorochelon soriana* shares with *Fon. cassouleti* the pattern of the first two neurals, whereas the perpendicular shape of the humero-pectoral sulcus and the shape of the suprapygals (first embraces the second lenticular one; Appendix, Fig. 17) place this taxon in a more derived position.

Another clade is recovered in the stem of Testudinidae, containing *Hadrianus corsoni* (Leidy, 1871), "*Hadrianus*" *castrensis* (Bergounioux, 1935), "*Testudo*" *sharanensis* Yeh, 1965 and "*Testudo*" *eocaenica* (Hummel, 1935). This clade is supported by two synapomorphies (nine neural plates; posterior sulcus of vertebral 4 on neural 9) and one ambiguous synapomorphy (rounded humero-pectoral sulcus), whereas the more exclusive clade of "*Te.*" *sharanensis* and "*Te.*" *eocaenica* is supported by two synapomorphies [posterior sulcus of vertebral 5 crosses the suprapygal transversely (Appendix, Figs 17 and 19); no gular protrusion] and one ambiguous synapomorphy (femoro-anal sulcus forms an acute angle with the midline).

"*Testudo*" *eocaenica* is not recovered as a sister-taxon of *Pel. soriana* as otherwise suggested by Pérez-García et al. (2016). Also, "*Ha.*" *castrensis* was considered a nomen dubium by the same authors but our analysis shows that the material preserves enough anatomical information to allow a confident diagnosis and evaluation of its phylogenetic relationships. As such, and from a taxonomic point of view, our results suggest that either all these taxa should be considered as members of *Hadrianus*, or they all should have different generic combinations. Usually, most of these taxa have been considered as members of *Manouria* (e.g., Auffenberg, 1971, 1974; Crumly, 1984) but our

results show that they should be considered stem testudinids, distinct from *Manouria*. Also, note that this clade shows a wide distribution in the Northern Hemisphere (Palearctic and Nearctic) and is supported by two synapomorphies that might be correlated. However, the monophyly of this clade is recovered in all analyses herein. Regardless of their taxonomy, i.e., if they form a clade or not, these taxa are here identified as stem testudinids. Based on our taxon sampling, the origin of Pan-Testudinidae is located in the northern hemisphere and most probably in the Palearctic with an early expansion to the Nearctic.

The most derived stem testudinid in our analysis is *Oligopherus laticuneus* (Cope, 1873) from the Late Eocene of North America. The grouping of *Oli. laticuneus* with Testudinidae is supported by one unambiguous (flat epiplastral lip) and one ambiguous (coincidence between costo-peripheral suture and pleuro-marginal sulci) synapomorphy. It is excluded from Testudinidae by the absence of a posterior maxillary process (Appendix, Fig. 10), pleural 1 that touches the lateral parts of the nuchal (Appendix, Fig. 16) and narrow vertebrals compared to the pleurals. Originally described as a member of *Testudo*, Williams (1950) considered it as the most "primitive" member of the *Gopherus* lineage, a suggestion followed by most scholars (e.g., Hutchison, 1996). Our results find *Oli. laticuneus* unrelated to *Gopherus* but we note that all the stem nodes discussed above show low Bremer support (Fig. 3B).

Basal testudinids. The clade Testudinidae is supported by three synapomorphies in the total evidence analysis: the presence of a posterior maxillary process (Appendix, Fig. 10), pleural 1 lacking contact with the nuchal (Appendix, Fig. 16) and the wide vertebrals being almost equal with the pleurals. Several other characters of the cranium and shell are critical for placing taxa within Pan-Testudinidae [wide fissura ethmoidalis; inferior descending processes of the prefrontals; no contact between jugal and the pterygoid; anterior process of the pterygoid; ridge of the vomer; closed incisura columella auris; position of rib head on or very near the neural/costal suture in visceral view (Appendix, Fig. 18); no axillary and inguinal glands; no webbing between the digits]. However, these characters are revealed by common mapping and are not included in the list of synapomorphies for the basal nodes of Pan-Testudinidae because of the absence of cranial information and some missing shell characters in stem testudinids. As a consequence, the numerical support of Testudinidae is decreased with the inclusion of these fossil taxa with missing characters from the shell. This is a usual outcome of the inclusion of incomplete fossils in phylogenetic analyses (Escapa and Pol, 2011; and references therein) and was noted in the first total evidence analysis of Testudines by Shaffer et al. (1997).

The basal taxa within Testudinidae include *Manouria*, "*Geochelone*" *costaricensis* and *Gopherus* in successive positions. The grouping of "*Geochelone*" *costaricensis* Segura Paguaga (1944) with the remaining Testudinidae is supported by four synapomorphies [octagonal neural 4; rectangular neural 5; posterior sulcus of vertebral 5 crosses the suprapygal transversely (Appendix, Figs 17 and 19); subrounded to straight anterior lobe] but the absence of an epiplastral lip and the hexagonal neurals 1 and 2 (with short postero-lateral sides) place this taxon in a basal position. Our results indicate that "*Geo*." *costaricensis* may not be related to South American tortoises as otherwise suggested by Auffenberg (1971), Bramble (1971) and indirectly by Crumly (1984). Auffenberg (1971) suggested that it could be related to an Asian genus (e.g., *Indotestudo*) based on an overlap of the pectoral scutes on the entoplastron, but this is not confirmed by our total evidence results. The position of this taxon is one of the few affected in the IW analysis. Weighting against homoplasy places "*Geo*." *costaricensis* within *Indotestudo*, as Auffenberg (1971) suggested. Future work on the affinities of this apparently important taxon, as well as the discovery of additional specimens from Central America, would be very important to document the early evolution and biogeography of testudinids. Regardless, the taxonomy of "*Geo*." *costaricensis* needs revision and this taxon probably needs to be included in a separate genus.

All other derived testudinids are members of the clade Testudininae, which includes both Testudona and Geochelona. Testudininae is supported by five synapomorphies (no foramen carotico-pharyngeale; strongly interdigitated suture between surangular and dentary; cervical scute longer than wide; clearly convex epiplastral lip; radius completely separated from the distal carpals).

Basal Geochelona. In a basal position within Geochelona (see definition above), we have recovered an extinct clade of unusual geographical distribution that contains Nearctic (*Stylemys nebrascensis* Leidy, 1851 and *Hesperotestudo* spp.), Palearctic [western: "*Ergilemys*" *bruneti* de Broin, 1977, *Cheirogaster maurini* Bergounioux, 1935 and *Taraschelon gigas* (Bravard, 1844); south-western: *Gigantochersina ammon* (Andrews 1906); eastern: *Ergilemys insolitus* (Matthew and Granger, 1923)] and Afrotropical (*Impregnochelys pachytestis* Meylan and Auffenberg, 1986 and *Namibchersus namaquensis* (Stromer, 1926) taxa. They are placed within Geochelona by the presence of contact between marginal 6 and pleural 3 and their basal position within Geochelona is based on

the presence of a cervical scute. This clade is supported by three synapomorphies (well-developed anterior and posterior buttresses that make clear contact with the costals, gulars covering the anterior area of the entoplastron). The clade containing *St. nebrascensis*, "*Erg*." *insolitus*, *Ch. maurini* and *Tar. gigas* (in successive positions) is supported by two synapomorphies (neurals 4 and 5 hexagonal with short antero-lateral sides), the clade of "*Erg*." *insolitus* by two (no coincidence between costo-peripheral suture and pleuro-marginal sulci; contact between marginal 2 and vertebral 1), whereas the sister-group relationship of *Ch. maurini* and *Tar. gigas* is supported by three synapomorphies (nuchal notch present; no cervical scute; rounded humero-pectoral sulcus).

The remaining taxa form a separate clade supported by ambiguous synapomorphies in some trees only [pleural 1 touches the lateral parts of the nuchal (Appendix, Fig. 16); short major trochanter of the humerus]. The grouping of the Afrotropical *Imp. pachytestis* with *Gi. ammon* is supported by two synapomorphies of the shell (gular protrusion; humeral equal or shorter than gulars), whereas the grouping of *He. crassiscuttata* and *He. bermudae* is supported by three [extent of median maxillary ridge (Appendix, Fig. 9); short cervical scute; contact between marginals 10 with vertebral 5].

The low support values (Fig. 3B), coupled with the fact that despite a cosmopolitan distribution not a single extant taxon is included, cast doubt on the monophyly of this group. In the morphological analysis (Fig. 3A) most of these taxa are again grouped together, except for the clade *Ergilemys* + *Cheirogaster* + *Taraschelon* that is placed within Testudona. Some less inclusive, geographically restricted clades could be potentially monophyletic but the best current estimate is to consider all these taxa as Testudinidae *incertae sedis*. The phylogenetic position of these taxa should be further explored, as it would have important implications on the taxonomy, palaeobiogeography and evolutionary history of Testudinidae.

Some additional important conclusions are as follows. The strongly supported sister-group relationship of *Cheirogaster maurini* and *Taraschelon gigas* suggests that perhaps the generic distinction proposed by Pérez-García and Vlachos (2014) and Pérez-García (2016) is unnecessary. Both the geographical and the temporal proximity would concur with this view. As such, previous referrals of *gigas* to *Cheirogaster* are justified (e.g., de Broin, 1977; Lapparent de Broin, 2001, 2002; among others) and *Taraschelon* Pérez-García, 2016 can be considered as a junior synonym of *Cheirogaster* Bergounioux, 1935.

Our results also suggest that *Stylemys* and *Hesperotestudo* may not be related to the gopher tortoises. This finding would challenge the traditionally accepted hypothesis that North American tortoises share a more recent common ancestor than other testudinids (e.g., Hay, 1908; Williams, 1950; and references therein; but see Bramble, 1971; Crumly, 1994 and Meylan and Sterrer, 2000 for alternatives). In all cases, biogeography and the presence of a medial ridge on the ventral side of the premaxillae (present in *Gopherus* and *Stylemys*; absent in *Hesperotestudo*) was demonstrated as clear evidence to support the close relationship of these taxa. However, this character alone fails to unite them under expanded sampling. Crucial for the interpretation of this result is the recovered position of *Ol. laticuneus* in the stem (see above) as that taxon also possesses a medial ridge in the premaxillae. As in our analysis this taxon is placed on the stem of Testudinidae, the presence of this character in *Gopherus* and *Stylemys* is optimized as homoplastic.

Also, our analysis identifies *Gigantochersina ammon* and *Cheirogaster maurini* as members of Testudinidae, therefore being the oldest crown tortoises, as Holroyd and Parham (2003) suggested. The placement of *Gi. ammon* and *Ch. maurini* within Testudinidae indicates a rapid diversification and wide distribution of the main testudinid clades well before the Late Eocene.

Derived Geochelona. With the exception of the Indian Ocean tortoises (herein represented only by *Astr. radiata*) the remaining extant geochelonans form a derived clade within Geochelona that includes several extinct taxa as well. This clade is supported by five synapomorphies [premaxilla/maxilla symphysis shorter than fossa nasalis (Appendix, Fig. 7); presence of premaxillary–maxillary cusp; elevated crista supraoccipitalis (Appendix, Fig. 13); absence of cervical scute, latissimus dorsi scar present]. The clade that contains the extant *Geochelone elegans*, *Centrochelys sulcata* and *Chelonoidis* spp. is supported by three synapomorphies (expanded opisthotic; keels in crista supraoccipitalis; triagonal ischial tubercle in pelvis). Within this clade we recover the extinct taxa "*Chelonoidis*" *gringorum* (Simpson, 1942) from the Early Miocene of South America and *Megalochelys atlas* (Falconer and Cautley, 1844) from the Plio-Pleistocene of Asia, joined together by two synapomorphies (gulars covering the anterior area of the entoplastron; reduced anal notch). Their sister-group relationship with *Centrochelys* is supported by two synapomorphies (gular protrusion present; concave epiplastral lip). The grouping of "*Chel*." *gringorum* and *Meg. atlas* is questioned by their far separated temporal and geographical distribution and we interpret this result with caution due to the limited information available for the two taxa. "*Chel*." *gringorum* is in need of revision and it is scored only from the holotype. *Meg. atlas* is poorly known and

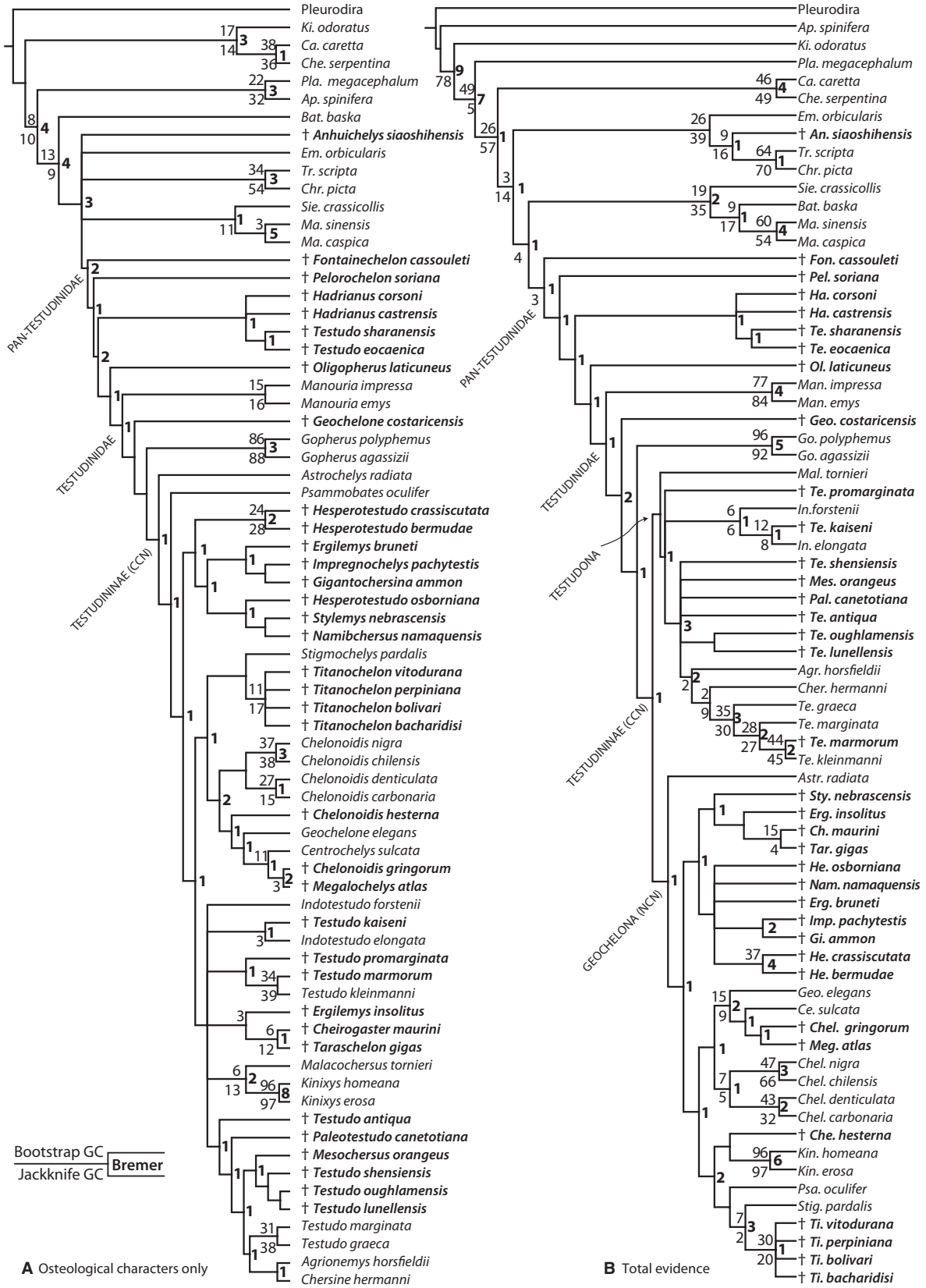

Fig. 3. A, strict consensus of the most parsimonious trees of extant and extinct taxa, using osteological characters. B, total evidence analysis of extant and extinct taxa. Extinct taxa are in bold and marked with a cross.

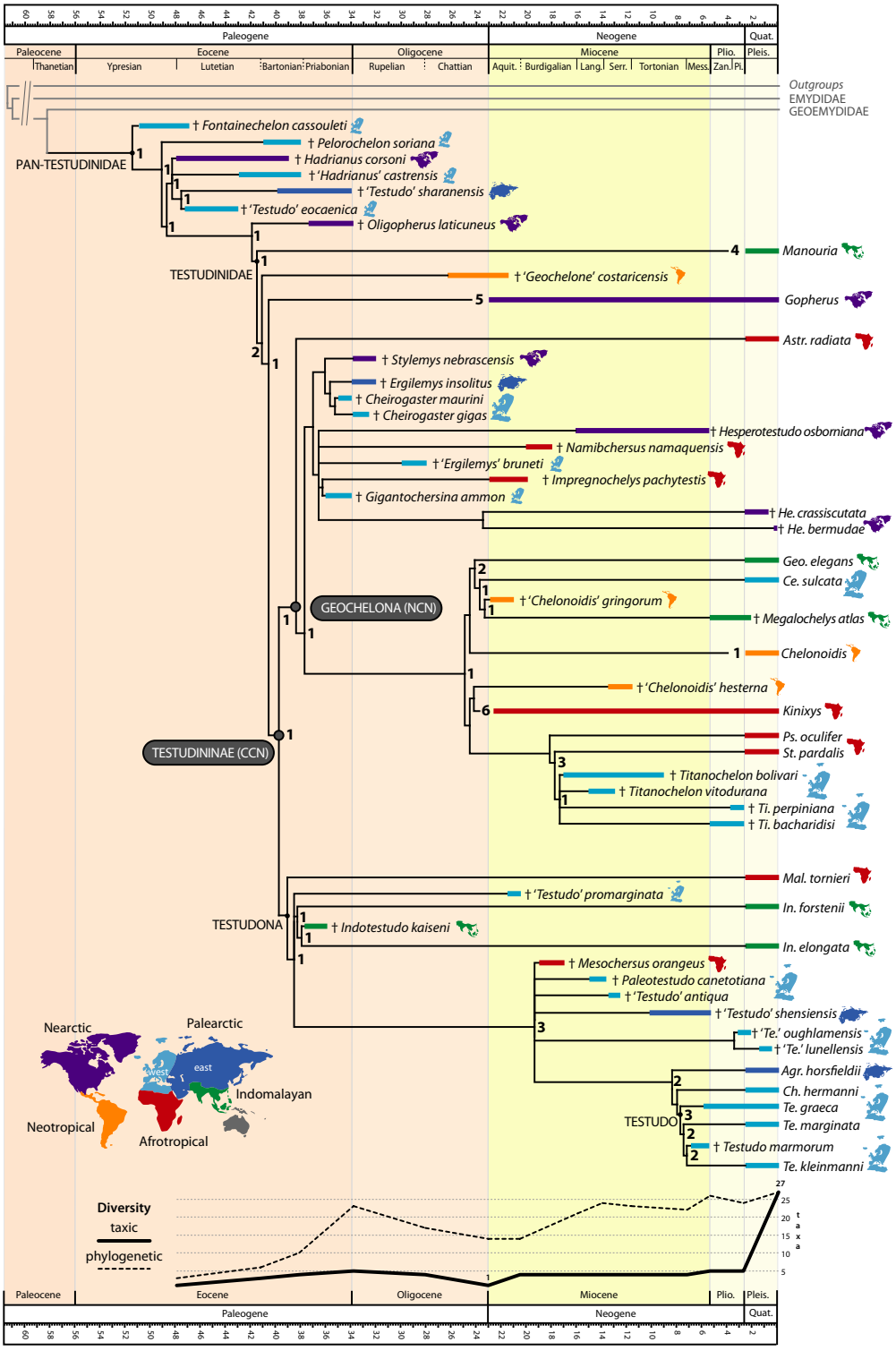

Fig. 4. Simplified time-calibrated phylogeny of Pan-Testudinidae based on the strict consensus tree of the total evidence analysis under equal weights. Bremer support values are in bold. Colours denote biogeographical realms shown as small maps for the printed. Extinct taxa are marked with a cross. Results of ghost lineage analysis are shown in the diagram below the tree including taxonomic diversity (as raw counts of taxa; solid line) and phylogenetic diversity (dashed line). [Color figure can be viewed at wileyonlinelibrary.com]

possibly the new information preliminarily reported by Hirayama et al. (2015) will shed light on the phylogenetic relationships of this gigantic tortoise.

The other main geochelonan clade, defined by the extant *Psammobates*, *Stigmochelys* and *Kinixys*, is supported by two synapomorphies (canalis praepalatinum absent; coronoid excluded from foramen alveolare inferius) and an ambiguous one (processus interfenestralis visible in ventral view). *Titanochelon* spp. from the Neogene of the western Palearctic are grouped with the extant Afrotropical *Stigmochelys* by three synapomorphies (processus pterygoideus externus at the same level with the foramen palatinum posterius; keels present in crista supraoccipitalis; long crista supraoccipitalis). The grouping of *Titanochelon* with the Palearctic/African large tortoise *Ce. sulcata* (e.g., Lapparent de Broin, 2001, 2002; Luján et al., 2014) would imply at least 12 additional steps. The monophyly of *Titanochelon* is supported by five synapomorphies [V-shaped basisphenoid (Appendix, Fig. 12); anterior and posterior buttresses well developed; no contact between inguinal and femoral scutes; reduced anal notch). Our results further show that the European giant tortoises from the Neogene (*Titanochelon*) are distinct from the Palaeogene ones (*Cheirogaster*) (as suggested by Pérez-García and Vlachos, 2014) and that they are possibly members of a larger clade of Afrotropical origin. The latter would imply dispersal from Africa to Europe prior to the Miocene and a turnover of Palearctic large tortoise faunas between the Palaeogene (*Cheirogaster*, *Ergilemys*) and Neogene (*Titanochelon*). Forcing a sister-group relationship between *Titanochelon* and *Cheirogaster* would imply at least three additional steps in a derived position within Geochelona; this placement would be further problematic because it would imply the existence of numerous ghost lineages of extant Geochelona originating in the Late Eocene. The placement of *Titanochelon* in a basal position with *Cheirogaster* would imply at least 12 more steps.

Another extinct taxon within this clade is the Miocene "*Chelonoidis*" *hesterna* from South America, grouped with the African *Kinixys* by three synapomorphies [neural 1 hexagonal with short postero-lateral sides; posterior sulcus of vertebral 5 coincides with pygal/suprapygal suture (Appendix, Figs 17 and 19); flat dorsal side of epiplastra]. Again, this unusual grouping should be interpreted with caution as the carapacial characters in *Kinixys* are altered secondarily by the presence of the carapacial hinge (see above). These results nevertheless suggest that the South American/Neotropical tortoises might not be monophyletic: this has been suggested by Crumly (1984) based on morphology and also recovered in a recent molecular analysis (Rodrigues and Diniz-Filho, 2016).

Testudona. This clade is supported by eight synapomorphies [elongate prootic; dorsal projection in maxilla/premaxilla suture; presence of premaxillary–maxillary cusp; for. jug. posterius in exoccipital/opisthotic suture; coronoid excluded from for. alv. inferius; elevated crista supraoccipitalis (Appendix, Fig. 13); coronoid excluded from foramen alveolare posterius; pleural 1 touches the lateral parts of the nuchal (Appendix, Fig. 16)] and an ambiguous one (posterior sulcus of vertebral 5 coincides with suprapygal/pygal suture; Appendix, Fig. 19). The members of Testudona are also characterized by the absence of contact between pleural 3 and marginal 6 but the optimization of this character is ambiguous (see above and Fig. 2B). The basal-most extinct taxon within Testudona is "*Testudo*" *promarginata* Reinach, 1900 from the Early Miocene of Germany, recovered between *Mal. tornieri* and derived testudonans. This grouping is supported by two synapomorphies (no gular protrusion; gulars covering the anterior area of the entoplastron) and three ambiguous ones (border of premaxillae projects ventrally; opisthotic expanded but does not touch the pterygoid; coronoid process as high as the dentary). The humerals that are much longer medially than the gulars distinguish "*Testudo" promarginata* from more derived testudonans (*Indotestudo* + Pan-*Testudo*). The *Indotestudo* clade is supported by the advanced position of the humero-pectoral sulcus coinciding with the posterior side of the entoplastron and the wavy humero-pectoral sulcus as an ambiguous synapomorphy. Within this clade we recover the extinct taxon "*Testudo*" *kaiseni* Gilmore, 1931, which is joined with *Ind. elongata* by the humero-pectoral sulcus that crosses the entoplastron and two ambiguous synapomorphies [more symmetrical nuchal (Appendix, Fig. 15); humerals equal or smaller with the gulars]. The recovery of "*Te*." *kaiseni* as a member of crown *Indotestudo* confirms the findings of Crumly (1984) and helps to trace the origin of Testudona back to as early as the Late Eocene of Asia. This age is significantly older than the conservative age provided by Parham et al. (2006) for this clade (Late Miocene, 15 Ma) and fills most of the ghost lineage with the oldest member of the "*Geochelone* complex" (Parham et al., 2006:60). However, a long ghost lineage persists for Pan-*Testudo* and for "*Testudo" promarginata*. The Middle to Late Eocene split of testudonans into Indomalayan and Palearctic lineages suggests that it was driven by the uplift of the Himalayans (see Yin, 2006, and references therein for geotectonic evolution).

The Pan-*Testudo* clade is supported by one synapomorphy (narrow gulars) and three ambiguous ones (short cervical scute; not perpendicular humero-pectoral sulcus; acute angle of the femoro-anal sulcus). *Testudo* is supported by four synapomorphies

(humerals longer than gulars; presence of a plastral hinge between the hypoplastra and xiphiplastra; omega-shaped femoro-anal sulcus; presence of latissimus dorsi scar). Several extinct taxa ("*Testudo*" *shensiensis* Wiman, 1930, *Mesochersus orangeus* Lapparent de Broin, 2003, *Paleotestudo canetotiana* Lartet, 1851, "*Testudo*" *antiqua* Bronn, 1831) are placed in the stem of *Testudo*, all being basal to the extant *Agrionemys horsfieldii* and *Chersine hermanni*. Also, in the stem of *Testudo*, a clade is formed by "*Testudo*" *oughlamensis* Gmira et al., 2015 and "*Testudo*" *lunellensis* Almera and Bofill, 1903 based on two ambiguous synapomorphies (humerals longer than gulars; anals longer than femorals). As there is no coincidence between the hypo-xiphiplastral suture and femoro-anal sulcus, "*Te*." *oughlamensis* was scored as having no hinge. Even if we follow Gmira et al. (2013) and score the hinge as present, "*Te*." *oughlamensis* holds its position outside *Testudo*. The only extinct taxon found within *Testudo* is *Testudo marmorum* Gaudry, 1862, as a sister group of *Te*. *kleinmanni* supported by four synapomorphies [pleural 1 covering the lateral parts of the nuchal (Appendix, Fig. 16); narrow anterior half of vertebral 1; no protrusions in the peripherals; humero-pectoral sulcus posterior to the entoplastron], confirming the position recovered by Vlachos and Tsoukala (2016).

Diversity

Even if our taxon sampling is by far the most extensive relative to previous works, it is still incomplete for providing robust estimates of diversity changes among pan-testudinids throughout the Cenozoic. In particular, only five extinct species per stage are represented in our matrix (Fig. 4, bottom). Ghost lineage analysis of the data set (Norell, 1992; Pol and Leardi, 2016, and references therein) nevertheless reveals a preliminary phylogenetic diversity pattern (dashed line in Fig. 4, bottom). In each period, the true pan-testudinid diversity should be minimally five times higher than our current sampling. Taxonomic diversity increases in the Late Eocene with a minimum estimate of 23 taxa. This is followed by a gradual diversity decrease until the Early Miocene and increase again in the Middle Miocene.

Body size analysis

The results are given in detail in Fig. 5 and in the Supporting Information, S5 and S6. These include three sets of data; the size of terminal taxa (midline carapacial length in cm; $n = 115$, min = 12, max = 175, mean = 44.55652, SD = 28.34289), the average estimated plesiomorphic carapacial size (PS) (in cm; $n = 115$, min = 20, max = 115, mean = 41.36522, SD = 20.34541) and the age (in Ma) of the terminal taxa. Neither the body size of terminal taxa nor the reconstructed PS show normal distribution (Shapiro–Wilk test: $2.49e^{-11}$ and $1.88e^{-10}$, respectively), whereas the probability that these two sets are correlated is high (Spearman's r_s probability to be uncorrelated: $2.64e^{-34}$). The differences of the variances between the two sets is significant (Levene's test for homogeneity of variance P(same) = 0.001635). To provide a graphical model to distinguish those significant cases, we performed a regression analysis (Supporting Information, Fig. SF6) with a LOESS smoothing line. Points that were placed outside the 95% confidence area (CA) are candidates of potential significant difference. As the reconstruction of the size evolution could depend on the topology, we only discuss uncontroversial size trends for the main pan-testudinid clades with strong support. The maximal midline carapace length of several extinct taxa was based on single or few specimens and therefore the extent of their size variation is unknown. Although the topologies of EW and IW (Supporting Information, Files S7 and S8) are quite different in the placement of poorly supported clades, the main trends of body size evolution for Testudona and Geochelona are identical under the two weighting strategies with the exception of a few cases of autapomorphic giantism/nanism events.

Our analysis shows that PS of the major clades of Pan-Testudinidae is medium (Fig. 5) and specifically 37 cm long for the *Fon. cassouleti* clade, 42–46 cm long for the other clades in the stem of Testudinidae and 38–39 cm long within Testudinidae (Fig. 5). Some Eocene stem-testudinids have retained their size within this range (e.g., "*Ha*." *castrensis*, "*Te*." *sharanensis*), whereas others showed a minor ("*Te*." *eocaenica*; *Ha. corsoni*) or significant increase (*Pe. soriana*), which are optimized as autapomorphic giantism events. At the base of crown Testudinidae, body size increased (*Ma. emys*) or decreased (*Ma. impressa*; "*Geo*." *costaricensis*) significantly, whereas *Gopherus* retains its PS. The oldest events of giantism in Testudinidae are identified in the Late Eocene of Africa (*Gi. ammon*) and Early Oligocene of Europe (*Cheir. gigas*) (Fig. 5 and Supporting Information, File S6B). The giantism event of the Late Eocene coincides with the first peak in the diversity of the clade. Geochelonans evolved giant sizes several times independently, during the Miocene of Africa (*Nam. namaquensis*), North America (*He. osborniana*) and Europe (*Titanochelon*) as well as during the Pliocene of Europe (*Titanochelon*) and Asia (*Meg. atlas*) and Pleistocene of North and South America (*He. crassiscutata*; Galápagos tortoises). Within Geochelona, we notice the greatest degree of variation in body size and this group also includes the largest tortoise known (*Meg. atlas*). Some geochelonans, however, went through autapomorphic nanism in the Pleistocene of North America and Africa (*He. bermudae*; *Kinixys*; *Psa. oculifera*).

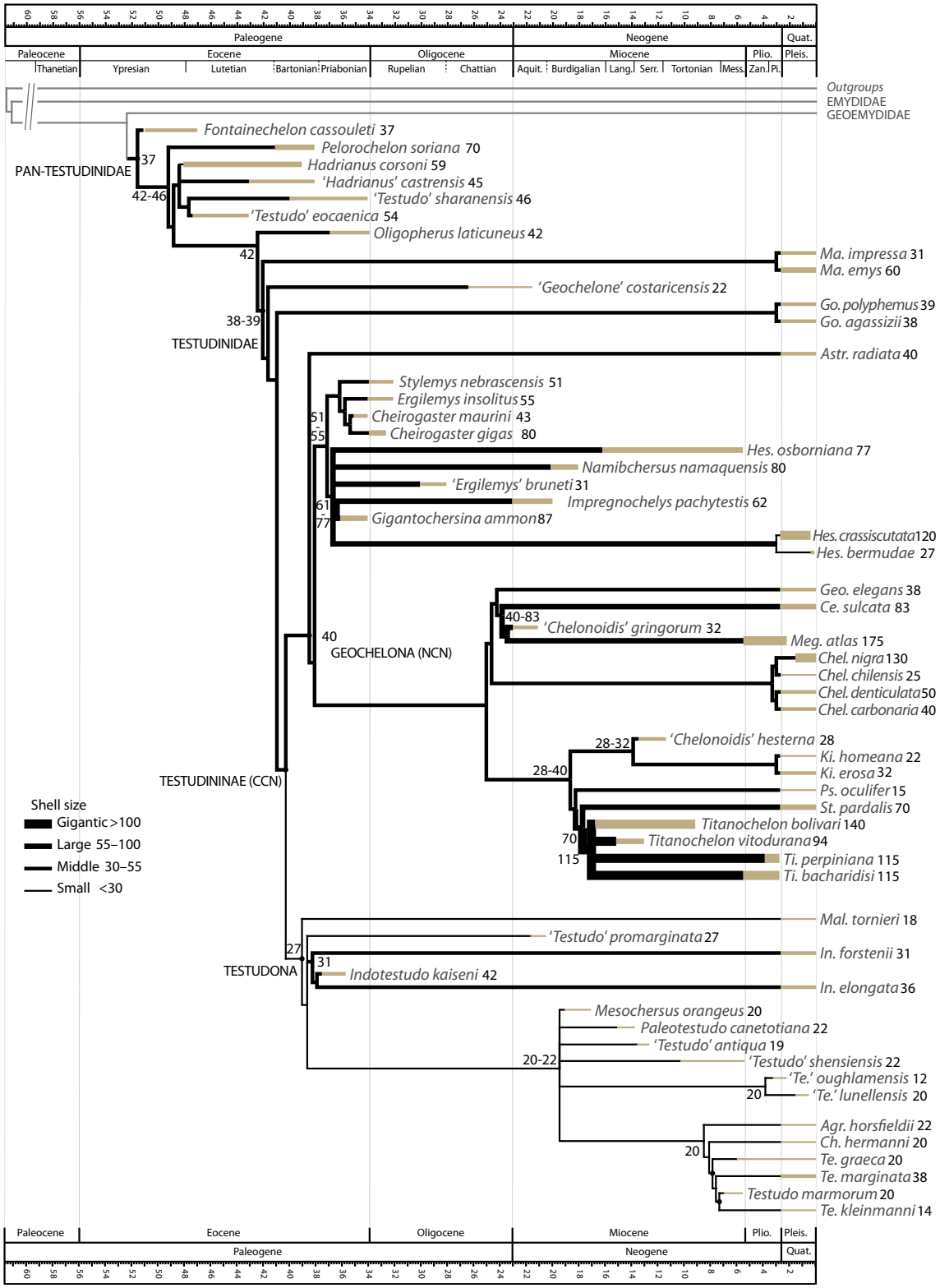

Fig. 5. Body size evolution of Pan-Testudinidae. Numbers on nodes indicate the reconstructed plesiomorphic carapace size for the clade, whereas next to species, indicate average carapace size (in cm). Thickness of the lines corresponds to carapace size. Nodes without numbers retain the plesiomorphic body size of the previous ancestral node. Giantism has evolved several times independently in stem, basal and derived testudinids. Geochelonans show the greatest variety of body sizes and include both the largest and the smallest species of known Pan-Testudinidae. Testudonans, by contrast, evolved markedly decreased body size. [Color figure can be viewed at wileyonlinelibrary.com]

The Testudona clade is characterized by an initial important decrease in size (Fig. 5) and further decrease in the majority of testudonans with the most extreme reduction in *Mal. tornieri*, *Te. kleinmanni* and "*Te.*" *oughlamensis* (Fig. 5 and Supporting Information, File S6). Exceptions to this trend include the slight body size increase in *Indotestudo* spp. and *Te. marginata*, although in both cases the increase is primarily due to the elongation of the carapace (especially that of the posterior part).

Discussion

Phylogeny, diversification and taxonomy

The total evidence matrix presented here is the most comprehensive global phylogenetic data set of Pan-Testudinidae and represents a significant advancement for the placement of extinct taxa. Parsimony analysis of this matrix revealed significant differences between morphological and molecular topologies but this is largely due to the specialized morphology of some taxa and not the quality of the morphological data itself.

In contrast to previous studies, the total evidence analysis recovered a widely distributed and relatively diverse stem lineage of testudinids including mostly Eocene taxa from the Palearctic and Nearctic. Other Palaeogene taxa are identified as members of crown Testudinidae, but their exact position within testudinids remains problematic. Palaeogene African tortoises (from both the Palaearctic and the Afrotropics) have somewhat ambiguous placement, but there is morphological support for the oldest taxa being close to Geochelona, a clade that shows its greatest modern diversity in Africa.

The origin of Testudininae and Testudona can be traced back to the Late Eocene in agreement with recent molecular estimates (Lourenço et al., 2012). All of the small-sized Palearctic Neogene testudinids sampled herein were recovered within Testudona with most extinct taxa being placed in the stem of *Testudo*. *Testudo marmorum* was identified as the only extinct species within *Testudo* indicating a relatively recent, Late Miocene, origin for crown *Testudo*, which is in accordance with the molecular clock analysis of Fritz et al. (2009). The Late Oligocene–Early Miocene estimate of Lourenço et al. (2012) is probably due to differences in the position of *Chersine hermanni* and *Agrionemys horsfieldi*.

Giant Neogene tortoises of the west Palearctic (*Titanochelon* spp.) are found deeply nested within Afrotropical Geochelona but not close to the only extant mainland giant tortoise, *Centrochelys sulcata*, unlike what has been previously proposed (Lapparent de Broin, 2002). Earlier large Palearctic taxa (*Cheirogaster maurini*, *Ch. gigas* and "*Erg.*" *bruneti*, represented by shells only) are best interpreted as a separate lineage in light of currently available data.

Ghost lineage analysis of the total evidence data set estimates high diversification during the Late Eocene and during the Middle to Late Miocene. Both peaks coincide with warm climatic conditions and the first is followed by a decline during the distinctly cooler Oligocene. However, we emphasize the necessity of testing these trends further through improved sampling of fossils.

In recent decades, molecular studies have tried to sort out the problem of the polyphyletic and paraphyletic use of "*Testudo*" and "*Geochelone*" due to the lack of consensus of testudinid relationships and nomenclature. The taxonomy of fossil taxa has been even more inconsistent. To introduce more stability, we provide definitions of new and converted clade names for the main derived clades of Testudinidae. Some extinct taxa may have to be referred to new genera to remain consistent with this phylogeny, but we nevertheless take a conservative approach and refrain from proliferating names, pending corroboration of our results by future analyses.

Body size evolution

The body size analysis identified independent evolution of giantism in multiple continental mainland taxa and therefore supports a recently proposed hypothesis that giantism in Testudinidae is not a result of insular effect (Itescu et al., 2014). Instead, we propose that giant forms are more probable colonizers of islands due to increased resistance to undernourishment.

The most surprising outcome of the reconstruction of body size in tortoises is the recovery of miniaturization in Testudona (< 30 cm carapace length). However, is difficult to confidently define the timing of this body size decrease. The clade originated in the Middle–Late Eocene based on molecular clocks (e.g., Lourenço et al., 2012) and the earliest known fossils (*Ind. kaiseni*) are larger than the reconstructed plesiomorphic body size of Testudona. By the Neogene, small body size had undoubtedly evolved but since our analysis identifies a long ghost lineage that spans the entire Oligocene the size decrease may have begun earlier. Potential Palearctic testudonan taxa from the Oligocene (e.g., "*Testudo*" *alba*, "*Testudo*" *corroyi* and "*Testudo*" *denozoti*; see Auffenberg, 1974, and references therein) are all small but these are yet to be included a phylogenetic analysis.

The analysis reveals no clear correlation between body size evolution and climate for the entire clade of Pan-Testudinidae. Increased taxon sampling or changes in the currently poorly supported phylogenetic position

of some fossil taxa may, however, demonstrate the role of cooling and warming in driving body size.

The evolution of giant size of the European *Titanochelon* spp. has been linked to the Middle Miocene Climatic Optimum (Böhme, 2003) and, although this hypothesis is impossible to test at the moment, it is consistent with our results. It has been recently proposed that further giantism in Late Miocene *Titanochelon* spp. and South-East Asian *Megalochelys* spp. may have been linked to climatic cooling and drying in the Late Miocene/Pliocene and/or reflect a dietary shift towards C_4 vegetation (Georgalis and Kear, 2013: 308).

Even if future studies reveal the role of climate in driving body size in pan-testudinids, we anticipate that correlation will be both negative and positive when the entire clade is considered. For instance, lowered temperature and increased seasonality is logically expected to shorten periods of annual growth and result in overall smaller body size but it may also trigger body size increase through the mechanism of gigantothermy (Paladino et al., 1990). The fact that extant Testudinidae do not conform to Bergman's rule (Angielczyk et al., 2015) alone indicates that the impact of climate on body size evolution is at best selective across the clade and is not an exclusive driving factor.

Acknowledgments

This work was financially supported by the joint program IKYDA 2014 between Greece (IKY) and Germany (DAAD) with the title "Phylogenetic relationships and evolutionary history of extinct European giant tortoises" and the Volkswagen Foundation. This project received further funding from a PICT-B-2334 (2016) grant from Agencia Nacional de Promoción Científica y Tecnológica, Argentina (FONCyT), and a Synthesys grant ES-TAF 2754 to E.V. and from the European Union's Seventh Framework programme for research and innovation under the Marie Skłodowska-Curie grant agreement No 609402 - 2020 researchers: Train to Move (T2M) to M.R. We thank the editor D. Stevenson, associate editor M. O'Leary and reviewers J. Parham, I. Danilov and R. V. Hill for carefully correcting the manuscript. We would like to thank numerous colleagues: W. G. Joyce, J. M. Mirande, D. Pol, J. Sterli, J. Parham, A. Pérez-García and A. Holley for valuable discussion, comments and for providing literature and photographs of specimens; C. Mehling (AMNH), G. Theodorou, S. Roussiakis, G. Lyras (AMPG), M. Moser (BSPG), E. Cioppi (IGF), E. Jimenez Fuentes (MCNUS), E. "Dudu" Ruigomez (MEF), D. Schwarz-Wings (MfN), J. Morales and P. Pérez Dios (MNCN), R. Allain and B. Battail (MNHN), R. van Zelst (NCB), M. Harzhauser, U. Göhlich and R. Gemel (NHMW), S. Scherrer (NWS), H. Furrer (PIMUZ), R. Boettcher and R. Schoch (SMNS), H.-D. Sues and A. Millhouse (USNM) for providing access to comparative collections; E. Tsoukala and M. Böhme for their guidance and support. The Willi Hennig Society sponsors the use of TNT software.

References

Ahl, H.E., 1927. Über einen weiteren Fund von *Testudo burchardi* E. Ahl aus Teneriffa. Zeitschrift der Deutschen Geologischen Gesellschaft 79, 445–447.

Angielczyk, K.D., Burroughs, R.W., Feldman, C., 2015. Do turtles follow the rules? Latitudinal gradients in species richness, body size, and geographic range area of the world's turtles. Journal of Experimental Zoology Part B: Molecular and Developmental Evolution, 324 (3), 270–294.

Auffenberg, W., 1963. Fossil testudinine turtles of Florida, genera *Geochelone* and *Floridemys*. Bulletin of the Florida State Museum 7 (3), 53–97.

Auffenberg, W., 1971. A new fossil tortoise, with remarks on the origin of South American Testudinines. Copeia, 10 6–117.

Auffenberg, W. 1974. Checklist of fossil land tortoises (Testudinidae). Bulletin of the Florida State Museum of Biological Sciences, 18 (3), 121–251.

Bell, T. 1828. Characters of the order, families, and genera of the Testudinata. Zoological Journal 3, 513–516.

Böhme, M., 2003. The Miocene climatic optimum: evidence from ectothermic vertebrates of Central Europe. Palaeogeogr. Palaeoclimatol. Palaeoecol. 195 (3), 389–401.

Bramble, D.M. 1971. Functional Morphology, Evolution, and Paleoecology of Gopher Tortoise. Doctoral dissertation, University of California, Berkley.

Bramble, D.M., Hutchison, J.H., 2014. Morphology, Taxonomy, and Distribution of North American Tortoises. In: Rostal, D.C., McCoy, E.D., Mushinsky, H.R., (Eds.), Biology and Conservation of North American Tortoises. John Hopkins University Press, Baltimore, USA, Vol. 1, pp. 1–12.

de Broin, F. 1977. Contribution à l"étude des Chéloniens: Chéloniens continentaux du Crétacé et du Tertiaire de la France. Mémoires du Muséum National d"Histoire Naturelle 38, 1–366.

Burke, R.L., Leuteritz, T.E., Wolf, A.J. 1996. Phylogenetic relationships of emydine turtles. Herpetologica 52 (4), 572–584.

Claude, J., Tong, H., 2004. Early Eocene testudinoid turtles from Saint-Papoul, France, with comments on the early evolution of modern Testudinoidea. Oryctos 5, 3–45.

Corsini, J.A., Böhme, M., Joyce, W.G., 2014. Reappraisal of *Testudo antiqua* (Testudines, Testudinidae) from the Miocene of Hohenhöwen, Germany. J. Paleontol. 88 (05), 948–966.

Crumly, C.R. 1982. A cladistic analysis of *Geochelone* using cranial osteology. Journal of Herpetology, 16 (3), 215–234.

Crumly, C.R. 1984. The evolution of land tortoises (Family Testudinidae). Ph.D. dissertation. Rutgers University, Newark.

Crumly, C.R., 1994. Phylogenetic systematics of North American tortoises (genus *Gopherus*): evidence for their classification. Fish and Wildlife Research 13, 7–32.

Crumly, C.R., Sánchez-Villagra, M.R., 2004. Patterns of variation in the phalangeal formulae of land tortoises (Testudinidae): developmental constraint, size, and phylogenetic history. Journal of Experimental Zoology Part B: Molecular and Developmental Evolution 302 (2), 134–146.

Delfino, M., Chesi, F., Fritz, U., 2009. Shell morphology of the Egyptian tortoise, Testudo kleinmanni Lortet, 1883, the osteologically least-known Testudo species. Zoological Studies 48 (6), 850–860.

Ernst, C.H., Barbour, R.W. 1989. Turtles of the world. Smithsonian Inst. press, Washington.

Escapa, I.H., Pol, D., 2011. Dealing with incompleteness: new advances for the use of fossils in phylogenetic analysis. Palaios 26, 121–124.
Franz, R. 2014. The Fossil Record for North American Tortoises. In: Rostal, D.C., McCoy, E.D., Mushinsky, H.R., (Eds.), Biology and Conservation of North American Tortoises. John Hopkins University Press, Baltimore, USA, Vol. 2, pp. 13–24.
Fritz, U., Bininda-Emonds, O.R., 2007. When genes meet nomenclature: tortoise phylogeny and the shifting generic concepts of *Testudo* and *Geochelone*. Zoology 110 (4), 298–307.
Fritz, U., Harris, J.D., Fahd, S., Rouag, R., Gracià Martinez, E., Giménez Casalduero, A., Široký, P., Kalboussi, M., Jdeidi, T., Hundsdörfer, A.K., 2009. Mitochondrial phylogeography of *Testudo graeca* in the Western Mediterranean: old complex divergence in North Africa and recent arrival in Europe. Amphibia– Reptilia 30, 63–80.
Gaffney, E.S., 1979. Comparative cranial morphology of the recent and fossil turtles. Bulletin of the American Museum of Natural History 164, 65–375.
Gaffney, E.S., Meylan, P.A., 1988. A phylogeny of turtles. The phylogeny and classification of the tetrapods, 1, 157–219.
Georgalis, G.L., Kear, B.P., 2013. The fossil turtles of Greece: an overview of taxonomy and distribution. Geobios 46 (4), 299–311.
Gerlach, J., 2001. Tortoise phylogeny and the "*Geochelone*" problem. Phelsuma 9 (suppl A), 1–24.
Gmira, S., Broin, F.D.L.D., Geraads, D., Lefèvre, D., Mohib, A., Raynal, J.P., 2013. Les tortues du Pliocène d"Ahl al Oughlam (Casablanca, Maroc) et de localités Mio-Pliocènes avoisinantes. Geodiversitas 35 (3), 691–733.
Goloboff, P.A., 2014. Extended implied weighting. Cladistics 30 (3), 260–272.
Goloboff, P.A., Farris, J.S., Källersjö, M., Oxelman, B., Szumik, C.A., 2003. Improvements to resampling measures of group support. Cladistics 19 (4), 324–332.
Goloboff, P.A., Farris, J.S., Nixon, K.C., 2008. TNT, a free program for phylogenetic analysis. Cladistics 24 (5), 774–786.
Gould, G.C., MacFadden, B.J., 2004. Chapter 17: gigantism, dwarfism, and Cope's rule: "Nothing in evolution makes sense without a phylogeny". Bull. Am. Mus. Nat. Hist. 21, 9–237.
Gray, J.E. 1870. Supplement to the catalogue of shield reptiles in the collection of the British Museum, pt. 1, Testudinata (tortoises). Taylor and Francis, London.
Guillon, J.M., Guéry, L., Hulin, V., Girondot, M., 2012. A large phylogeny of turtles (Testudines) using molecular data. Contributions to Zoology 81 (3), 147–158.
Hammer, Ø., Harper, D.A.T., Ryan, P.D. 2009. PAST-PAlaeontological STatistics, ver. 1.89. University of Oslo, Oslo, 1–31.
Hay, O.P. 1908. The fossil turtles of North America. Carnegie Institution of Washington, Washington, DC.
Hervet, S. 2003. Le groupe" *Palaeochelys* sensu lato–*Mauremys*" dans le contexte systématique des Testudinoidea aquatiques du Tertiaire d"Europe occidentale: Apports à la biostratigraphie et à la paléobiogéographie. Doctoral dissertation, Paris, Muséum national d'Histoire naturelle.
Hirayama, R., 1985. Cladistic analysis of batagurine turtles (Batagurinae: Emydidae: Testudinoidea); a preliminary result. Studia Geológica Salmaticensia Volumen Especial 1: Studia Palaeocheloniologica 1, 141–157.
Hirayama, R., Sonoda, T., Takai, M., Htike, T., Thein, Z.M.M., Takahashi, A. 2015. *Megalochelys*: gigantic tortoise from the Neogene of Myanmar. PeerJ PrePrints 3:e961v1, https://doi.org/10.7287/peerj.preprints.961v1.
Holroyd, P.A., Parham, J.F., 2003. The antiquity of African tortoises. J. Vertebr. Paleontol. 23 (3), 688–690.
Hutchison, J.H. 1996. Testudines. The Terrestrial Eocene-Oligocene Transition in North America. Cambridge University Press, Cambridge, 337–353.
Hutterer, R., Casañas, F.G.T., Martínez, N.L., Michaux, J., 1997. New chelonian eggs from the Tertiary of Lanzarote and Fuerteventura, and a review of fossil tortoises of the Canary Islands (Reptilia, Testudinidae). Vieraea: Folia scientarum biologicarum canariensium 26, 139–161.
Itescu, Y., Karraker, N.E., Raia, P., Pritchard, P.C., Meiri, S., 2014. Is the island rule general? Turtles disagree. Glob. Ecol. Biogeogr., 23 (6), 689–700.
Joyce, W.G., Bell, C.J., 2004. A review of the comparative morphology of extant testudinoid turtles (Reptilia: Testudines). Asiatic Herpetological Research 10, 53–109.
Joyce, W.G., Parham, J.F., Gauthier, J.A., 2004. Developing a protocol for the conversion of rank-based taxon names to phylogenetically defined clade names, as exemplified by turtles. J. Paleontol. 78 (05), 989–1013.
Joyce, W.G., Parham, J.F., Lyson, T.R., Warnock, R.C.M., Donoghue, P.C.J., 2013. A divergence dating analysis of turtles using fossil calibrations: an example of best practices. J. Paleontol. 87, 612–634.
Kindler, C., Branch, W.R., Hofmeyr, M.D., Maran, J., Vences, M., Harvey, J., Hauswaldt, J.S., Schleicher, A., Stuckas, H., Fritz, U., 2012. Molecular phylogeny of African hinge-back tortoises (*Kinixys*): implications for phylogeography and taxonomy (Testudines: Testudinidae). J. Zoolog. Syst. Evol. Res. 50 (3), 192–201.
Lamb, T., Lydeard, C., 1994. A molecular phylogeny of the gopher tortoises, with comments on familial relationships within the Testudinoidea. Mol. Phylogenet. Evol. 3 (4), 283–291.
Lapparent de Broin, F.de., 2001. The European turtle fauna from the Triassic to the Present. Dumerilia 4 (3), 155–217.
Lapparent de Broin, F.de., 2002. A giant tortoise from the late Pliocene of Lesvos Island (Greece) and its possible relationships. Ann. Géol. Pays Hellén. 39, 99–130.
Lapparent de Broin, F.de., Bour, R., Perälä, J., 2006. Morphological definition of *Eurotestudo* (Testudinidae, Chelonii): first part. Annales de Paléontologie 92 (3), 255–304.
Le, M., Raxworthy, C.J., McCord, W.P., Mertz, L., 2006. A molecular phylogeny of tortoises (Testudines: Testudinidae) based on mitochondrial and nuclear genes. Mol. Phylogenet. Evol. 40 (2), 517–531.
Lee, M., 2001. Molecules, morphology and the monophyly of diapsid reptiles. Contributions to Zoology 70 (1), 1–17.
Leidy, J., 1871. Remarks on a fossil *Testudo* from Wyoming. Proc. Acad. Nat. Sci. Philadelphia 23, 154.
Linnaeus, C., 1758. Systema Naturae per Regna Tria Naturae, secundum Classes, Ordines, Genera, Species, cum Characteribus, Differentiis, Synonymis, Locis. Laurenti Salvii, Holmiae.
López-Jurado, L.F., Mateo, J.A., 1993. A new giant land tortoise from the Pliocene of Gran Canaria (Canary Islands). Revista Española de Herpetología 7, 107–111.
Lourenço, J.M., Claude, J., Galtier, N., Chiari, Y., 2012. Dating cryptodiran nodes: origin and diversification of the turtle superfamily Testudinoidea. Mol. Phylogenet. Evol. 62 (1), 496–507.
Luján, À.H., Alba, D.M., Fortuny, J., Carmona, R., Delfino, M., 2014. First cranial remains of *Cheirogaster richardi* (Testudines: Testudinidae) from the Late Miocene of Ecoparc de Can Mata (Vallès-Penedès Basin, NE Iberian Peninsula): taxonomic and phylogenetic implications. J. Syst. Paleontol. 12 (7), 833–864.
Luján, À.H., Delfino, M., Robles, J.M., Alba, D.M., 2016. The Miocene tortoise *Testudo catalaunica* Bataller, 1926, and a revised phylogeny of extinct species of genus *Testudo* (Testudines: Testudinidae). Zool. J. Linn. Soc. 178 (2), 312–342.
Mautner, A.K., Latimer, A.E., Fritz, U., Scheyer, T., 2017. An updated description of the osteology of the pancake tortoise *Malacochersus tornieri* (Testudines: Testudinidae) with special focus on intraspecific variation. J. Morphol., 278, 321–333.
McDowell, S.B., 1964. Partition of the genus Clemmys and related problems in the taxonomy of the aquatic Testudinidae. Proceedings of the Zoological Society of London 143(2), 239–278.
Meylan, P.A., Sterrer, W., 2000. *Hesperotestudo* (Testudines: Testudinidae) from the Pleistocene of Bermuda, with comments

on the phylogenetic position of the genus. Zool. J. Linn. Soc. 128 (1), 51–76.
Mirande, J.M., 2009. Phylogeny of the family Characidae (Teleostei: Characiformes): from characters to taxonomy. Neotropical Ichthyology 8 (3), 385–568.
Mirande, J.M., Jerep, F.C., Vanegas-Ríos, J.A., 2013. Phylogenetic relationships of the enigmatic *Carlastyanax aurocaudatus* (Eigenmann) with remarks on the phylogeny of the Stevardiinae (Teleostei: Characidae). Neotropical Ichthyology 11 (4), 747–766.
Norell, A.M. 1992. Taxic origin and temporal diversity: the effect of phylogeny. In: Novacek, M.J., Wheeler, Q.D. (Eds.), Extinction and Phylogeny. Columbia University Press, New York, pp. 89–118.
Paladino, F.V., O"Connor, M.P., Spotila, J.R., 1990. Metabolism of leatherback turtles, gigantothermy, and thermoregulation of dinosaurs. Nature 344 (6269), 858–860.
Parham, J.F., Macey, J.R., Papenfuss, T.J., Feldman, C.R., Türkozan, O., Polymeni, R., Boore, J., 2006. The phylogeny of Mediterranean tortoises and their close relatives based on complete mitochondrial genome sequences from museum specimens. Mol. Phylogenet. Evol. 38 (1), 50–64.
Perälä, J., 2002. The genus *Testudo* (Testudines: Testudinidae): phylogenetic inferences. Chelonii 3, 32–39.
Pérez-García, A., 2016. A new genus for "*Testudo*" *gigas*, the largest European Paleogene testudinid. J. Vertebr. Paleontol. 36 (1), e1030024.
Pérez-García, A., Vlachos, E., 2014. New generic proposal for the European Neogene large testudinids (Cryptodira) and the first phylogenetic hypothesis for the medium and large representatives of the European Cenozoic record. Zool. J. Linn. Soc. 172 (3), 653–719.
Pérez-García, A., Ortega, F., Jiménez Fuentes, E., 2016. Taxonomy, systematics, and diversity of the European oldest testudinids. Zool. J. Linn. Soc. 177 (3), 648–675.
Pol, D., Escapa, I.H., 2009. Unstable taxa in cladistic analysis: identification and the assessment of relevant characters. Cladistics 25 (5), 515–527.
Pol, D., Leardi, J.M. 2015. Diversity patterns of Notosuchia (Crocodyliformes, Mesoeucrocodylia) during the Cretaceous of Gondwana. In: Fernández, M., Herrera, Y. (Eds.), Reptiles Extinctos–Volumen en Homenaje a Zulma Gasparini. Publicación Electrónica de la Asociación Paleontológica Argentina 15(1), 172–186.
Pol, D., Norell, M.A., 2001. Comments on the Manhattan stratigraphic measure. Cladistics 17 (3), 285–289.
Rodrigues, J.F.M., Diniz-Filho, J.A.F., 2016. Ecological opportunities, habitat, and past climatic fluctuations influenced the diversification of modern turtles. Mol. Phylogenet. Evol. 101, 352–358.
Schoepff, J.D., 1795. Historia Testudinum iconibus illustrata. J.J. Palm., Erlangen, Germany.
Shaffer, H.B., Meylan, P., McKnight, M.L., 1997. Tests of turtle phylogeny: molecular, morphological, and paleontological approaches. Syst. Biol. 46 (2), 235–268.
Shaw, G. 1802. General Zoology, or Systematic Natural History. Volume III, Part I, Amphibia. G. Kearsley, London.
Sterli, J., 2010. Phylogenetic relationships among extinct and extant turtles: the position of Pleurodira and the effects of the fossils on rooting crown-group turtles. Contributions to Zoology 79 (3), 93–106.
Swingland, I.R., Klemens, M.W. 1989. The conservation biology of tortoises (Vol. 5). IUCN.
Takahashi, A., Otsuka, H., Hirayama, R., 2003. A new species of the genus *Manouria* (Testudines: Testudinidae) from the Upper Pleistocene of the Ryukyu Islands, Japan. Paleontological Research 7 (3), 195–217.
Tong, H., Li, L., Li, D.S., 2016. A revision of *Anhuichelys* Yeh, 1979, the earliest known stem Testudinidae (Testudines: Cryptodira) from the Paleocene of China. Vert. PalAsiat. 54 (2), 156–179.
Vlachos, E., 2015. The fossil chelonians of Greece. Systematics - evolution - stratigraphy - palaeoecology. Ph.D. thesis, Aristotle University of Thessaloniki, Greece.
Vlachos, E., Tsoukala, E., 2016. The diverse fossil chelonians from Milia (late Pliocene, Grevena, Greece) with a new species of *Testudo* Linnaeus, 1758 (Testudines: Testudinidae). Papers in Palaeontology 2 (1), 71–86.
Wilkinson, M., 1995. A comparison of two methods of character construction. Cladistics 11 (3), 297–308.
Williams, E.E. 1950. *Testudo cubensis* and the evolution of western hemisphere tortoises. Bull. Am. Mus. Nat. Hist., 95, 7–36. article 1.
Yin, A., 2006. Cenozoic tectonic evolution of the Himalayan orogen as constrained by along-strike variation of structural geometry, exhumation history, and foreland sedimentation. Earth Sci. Rev. 76 (1), 1–131.

Supporting Information

Additional Supporting Information may be found in the online version of this article:

File S1. Nexus file of the morphological taxon-character matrix. (.nex format)

File S2. List of synapomorphies of the phylogenetic analysis of extant taxa. (.pdf format)

File S3. Results of the iterPCR script on the different topologies produced by osteological characters alone and the topology based on molecules. (.pdf format)

File S4. List of morphological synapomorphies of the total evidence analysis of extant and extinct taxa. (.pdf format)

File S5. Table of carapace size measurements and ancestral size reconstruction of extinct and extant taxa. (.xlsx format)

File S6. Diagrams of size evolution. S6.A, scatter diagram of average size plotted against the plesiomorphic size for all taxa and nodes. Numbers refer to the node numbers of the strict consensus of the total evidence analysis (see File S4). S6.B, evolution of body size. In both cases a LOESS regression line is fitted. Data from Suppl. File S6. (.pdf format)

File S7. Results of the implied weights analysis. (.xlsx format)

File S8. The single tree obtained by the selected *K* value under implied weights. See text for more information. (.pdf format)

Appendix

List of characters used in the morphological phylogenetic analysis. References are abbreviated: **CR**, Crumly, 1984 matrix (additional acronym refers to the characters as defined therein; e.g., MEC refers to the character Medial Extent of Centralia in Crumly, 1984); **HI**, Hirayama, 1985 matrix; **GM**, Gaffney and Meylan, 1988 matrix (additional acronym refers to the clade name and number of synapomorphies therein; e.g., H6.3 refers to clade H6, synapomorphy 3); **MS**, Meylan and Sterrer, 2000 matrix; **GE**, Gerlach, 2001 matrix; **HE**, Hervet, 2003 matrix; **JB**, Joyce and Bell, 2004 matrix; **CT**,

Claude and Tong, 2004 matrix; **FLB**, Lapparent de Broin et al., 2006 matrix; **PV**, Pérez-García and Vlachos, 2014 matrix; numbers refer to the assigned character number in the mentioned paper, unless stated otherwise.

Cranial characters

0, Shape of the fissura ethmoidalis:

0 = narrow or closed, keyhole-shaped; 1 = very wide | *CR-WEF*; **JB1**; **CT9**

Definition: The definition of CR-WEF is roughly similar, but with the addition of an extra state for *Psammobates* (secondarily slightly narrow). *Psammobates* is not included in our ingroup. Based on our observations, the fissura of both *M. impressa* and *M. emys* is similar to the remaining testudinids, and therefore we follow the scoring of JB and CT.

Variation: In juveniles of *Chel. carbonaria*, the fissura is slightly smaller proportionally (but still not key-shaped). Also, due to the skull being more vaulted than elongated in juveniles, the fissura is placed more dorsally. By contrast, JB report larger fissura in juveniles as a result of reduced ossification.

1, Medial inflection of the inferior descending processes of the frontal:

0 = absent, or very small; 1 = present, well-developed, medial contact present or almost present | **JB2**; GE2 + GE3

Variation: The inferior descending processes in *Chel. carbonaria* are found as not in contact in all adult/subadult specimens. In three of 34 specimens the processes were very close but still no contact was present. However, in two of nine juvenile specimens the processes showed a medial contact, whereas in the others the condition was variable. In particular, in three of nine juvenile specimens the distance between the processes was very wide. Therefore, we agree with the view of JB that this character should not be subdivided due to changes in ontogeny. When various ontogenetic stages were known, we scored the character on adult individuals. This character is probably the same as GE3 (closure of sulcus olfactorius).

2, Frontal contribution to the orbital rim:

0 = present, no prefrontal/postorbital contact on dorsal surface; 1 = absent, frontal excluded from orbital rim by prefrontal/postorbital contact | GE1; **JB3**

Variation: Although in all specimens of *Chel. carbonaria* the frontal clearly participates in the orbital rim, we have found some differences that could be interpreted as due to sexual dimorphism. In 18 of 20 male individuals, the part of the orbital rim that is defined by the frontal is much smaller than the prefrontal part (in some cases only a tiny participation of the frontal is present). On the other hand, in eight of ten females individuals the frontal part is equal to or longer than the prefrontal part. Such variation has been noted in the juveniles as well, where at least three of eight juveniles had short frontal participation on the orbital rim. In the juvenile specimens, however, no indication on gender was available.

3, Median length of frontals, compared to the prefrontals (Fig. 6):

0 = prefrontals equal to or longer than frontals; 1 = frontals longer than prefrontals | **GE4** (modified)

Definition: This character is slightly modified from GE4, which was defined as "*median suture of the frontals more than twice as long as that between the prefrontals*" GE (p. 7). The reason is that we were unable to replicate the scorings of GE based on all the specimens that we have examined (regarding the double length of the frontals).

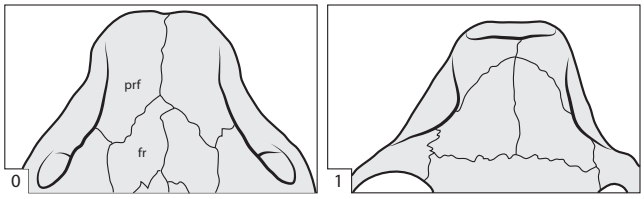

Fig. 6. Illustration of the different states of character 3: 0, frontals longer than prefrontals in *Chelonoidis nigra*; 1, frontals shorter than prefrontals in *Centrochelys sulcata*. Abbreviations: fr, frontal; prf, prefrontal.

Therefore, we choose a simpler approach of comparative median length of the two bones.

Variation: Although a degree of ontogenetic variation was observed on the specimens of *Chel. carbonaria*, this variation was between the limits of the character states as defined above.

4, Presence of prefrontal pits:

0 = absent; 1 = present | **CR-PP**

5, Contact between jugal and pterygoid:

0 = present, medial process of jugal well developed and touching the pterygoid; 1 = absent, medial process reduced | **JB4**

6, Contact between jugal and palatine:

0 = absent; 1 = present | **JB5**

7, Contact of the epipterygoid with the jugal:

0 = clearly absent; 1 = present, or almost present, epipterygoid forms a long lateral process that approaches the jugal | **JB6**; CT3

8, Contact of the inferior process of the parietal with the medial process of the jugal:

0 = absent; 1 = present | **JB7**

9, Contact of the inferior process of the parietal with the maxilla:

0 = absent; 1 = present | **JB8**

10, Extent of quadratojugal:

0 = quadratojugal well developed, firmly attached to jugal; 1 = quadratojugal present, contact with jugal lost; 2 = quadratojugal so heavily reduced that it appears to be absent in many skeletal specimens | **JB9** (modified) ORDERED

Definition: Our observations confirm the necessity of more than two states for this character as defined by JB. However, both in the description of JB, as well as based on our observations, state 1 is certainly intermediate between states 0 and 2. For this reason we argue for treating this character as an ordered one.

11, Contribution of jugal to the rim of upper temporal emargination:

0 = absent; 1 = present | **JB10**

12, Contact between the quadratojugal and the articular facet of the quadrate:

0 = absent; 1 = present, quadratojugal sends a process ventrally along the rim of the cavum tympani and touches the lateral edge of the articular facet | **JB11**

Variation: In all skulls of *Chel. carbonaria*, the quadratojugal does not touch the articular part of the quadrate. However, the shape of the posterior part of the quadratojugal is quite variable. There are cases that the quadratojugal sends two processes that circle the quadrate both dorsally and anteroventrally. In other cases the ventral process is not developed. This could be the result of slightly more extensive anteroventral emargination.

13, Contact between the parietal and the quadrate, partially covering the prootic dorsally:

0 = absent; 1 = present | **GE45**

Definition: Slightly re-phrased from GE45. This character appears for the moment as not informative, as it is found as present only in *Te. graeca*.

14, Shape to the prootic:

0 = anteroposteriorly short and wide; 1 = anteroposteriorly long and narrow | CR-PS (modified); MS20 (part)

Definition: CR-PS defined several states on this character regarding the shape of the prootic in dorsal view. We have been unable to replicate these states. Instead, we use a simpler coding to separate prootics that are rather short and wide (e.g., in *M. impressa*, *Go. polyphemus*) from prootics that are much longer and narrower (e.g., in *Chel. chilensis*, *Kin. erosa*). This character is not dependent on the development of the processus trochlearis oticum. Also it does not seem to be correlated with the size of the individual.

15, Contact between quadratojugal and maxilla:

0 = absent; 1 = present | **JB12**

16, Medial contact of the maxillae along the anterior margin of the jaw:

0 = absent; 1 = present | **JB13**

17, Height of the symphysis of the maxilla/premaxilla compared to the height of the fossa nasalis (Fig. 7):

0 = short, shorter than the height of fossa nasalis; 1 = short, shorter than the height of fossa nasalis, but with the development of a dorsal projection; 2 = high, taller than the height of fossa nasalis | **GE10** ORDERED

Definition: This character is slightly re-phrased from the original character GE10. Given that state 1 appears to be intermediate between states 0 and 2, this character was considered as ordered.

18, Size of the foramen orbito-nasale:

0 = small, less than 1/6 of orbit length; 1 = large, more than 1/6 of orbit length | CR-ONF; GE25 + 26; **JB14**; CT5.

Definition: JB14 (p. 60) point out the difficulty in scoring this character in testudinids due to the thin nature of the palatines. While we concur with this comment, our own observations on some testudinid taxa (e.g., *Chel. carbonaria*, *Chel. chilensis*, *Chel. denticulata*, *Te. graeca*, *M. impressa*, *Chel. nigra*, *Geo. radiata*, *Ce. sulcata*) still show the size of the foramen is small, as defined by state 0. The issue of fragmentation as pointed out by JB (p.60) was observed in *erosa* specimens, and those specimens were scored as unknown. In terms of scoring, the fragmentation could possibly influence the scores of specimens with large foramina, as the foramen might appear larger than it really is. In those with state 0 the scoring is clear. Even if some damage is present this means that the foramen is even smaller than the observed condition. This character has also been included in CT5, defined as medium-sized to large (0), minute (1), huge (2), with the reduction of the size being interpreted as a homoplasy. Here we follow the scoring of JB14.

Variation: In some specimens of *carbonaria* we noted differences in the size of the foramen between the left and right side (without any clear distribution), indicating that addition of extra intermediate steps should be considered with caution. Finally, the size of the foramen in juveniles of *carbonaria* shows more or less the same size as in the adults, thus being proportionally much larger in the juvenile specimens.

19, Contact between maxilla and vomer:

0 = present; 1 = absent, vomer separated from the maxilla by the premaxilla | CR-MVC; **JB15**

20, Size of the foramen palatinum posterius:

0 = large; 1 = small | **JB16**; CT10

21, Position of the pterygoid relative to foramen palatinum posterius (f.p.p.):

0 = pterygoid situated posterior to the f.p.p.; 1 = pterygoid situated posterior to the f.p.p., but sends a process anterior and lateral to the f.p.p | **JB17**

22, Epipterygoid participation in the trigeminal foramen:

0 = absent; 1 = present, epipterygoid clearly separates the parietal and pterygoid in lateral view | **JB18**

23, Degree of upper temporal emargination (Fig. 8):

0 = Broad contact (parietal–postorbital suture length equal to parietal–frontal); 1 = Reduced (parietal–frontal suture 1.5 times as long as parietal–postorbital); 2 = Narrow (parietal–frontal suture 3 times as long as parietal–postorbital) | **GE7** ORDERED

Definition: GE7 defined this character as a measure of the contact between the parietal and postorbital bones, as coded above.

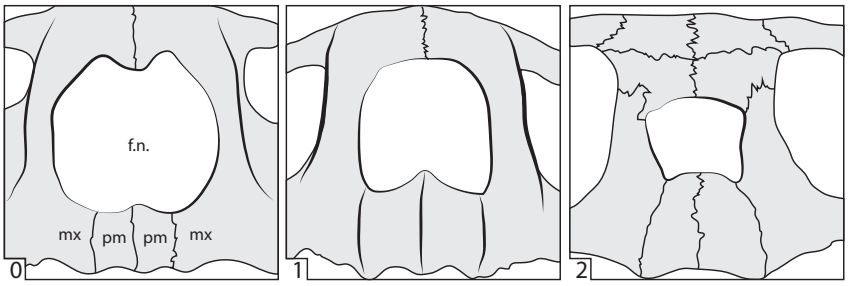

Fig. 7. Illustration of the different states of character 17, the height of the symphysis of the maxilla/premaxilla compared to the height of the fossa nasalis: 0, short in "*Testudo*" *hermanni*; 1, short, but with a dorsal projection in *Centrochelys sulcata*; 2, tall in *Indotestudo elongata*. Abbreviations: f.n., fossa nasalis; mx, maxilla; pm, premaxilla.

However, we find difficulties in replicating his scorings for some testudinids scored as 1 (e.g., *Ce. sulcata*, *St. pardalis*), whereas we were able to find specimens from some taxa scored by Gerlach as state 2 (e.g., *Te. graeca*) as having a more reduced contact. Based on our sampling, it seems clear that the scoring of this character as discrete states makes it difficult to clearly capture the entire morphological variation of the ingroup. Perhaps the best option for such a character would be to code it as a continuous. As we tentatively include this character with discrete coding, this character should be treated as an ordered one.

24, Shape of the labial ridge at the contact between the two premaxillae:
0 = notch present in the suture contacting the two premaxillae; 1 = the labial ridge is straight; 2 = the labial ridge projects ventrally or central premaxillary cusp present | ORDERED
Definition: This character refers to the outline of the labial ridge of the premaxillary symphysis in the anterior part of the triturating surface. In some outgroup taxa (e.g., *Ba. basca*, *Ma. caspica*, *Tra. scripta*) as well as in the ingroup (e.g., in some *Chel. chilensis* and *Chel. nigra*), the symphysis is notched and therefore convex dorsally. In other taxa (e.g., *Ste. odoratus*, *M. impressa*, *Go. polyphemus* among others), the symphysis is more or less straight. Finally, some taxa show a symphysis that projects ventrally with a roughly triangular process (e.g., *Kin. homeana* and *Kin. erosa*). As state 1 is clearly intermediate, this character is ordered.

25, Presence of a cusp in the premaxilla–maxilla suture:
0 = absent; 1 = present | GE9 (part); **CT11**
See comments on previous character (central maxillary cusp).

26, Presence of a circular or elliptical pit on the ventral side of the premaxillae:
0 = present; 1 = absent, ventral part of the premaxillae is flat |

27, Participation of palatine in the triturating surface of the upper jaw:
0 = absent; 1 = present | GE29; **JB28**

28, Participation of the vomer in the triturating surface of the upper jaw:
0 = absent; 1 = present | **JB29**

29, Presence of a median maxillary ridge on the triturating surface:
0 = absent; 1 = present | Based on CR-TR, CR-MPR, MS11, MS12, MS13, MS16, GE8, GE12, JB30, CT16, CT18 and on anatomical information from McDowell (1964) and Gaffney and Meylan (1988).

30, Presence of a lingual ridge on the triturating surface:
0 = absent; 1 = present |

31, Presence of a commissural ridge on the triturating surface (Fig. 9):
0 = absent; 1 = present |
Definition: The three characters mentioned above are discussed together. The definition, and more importantly the scoring, of

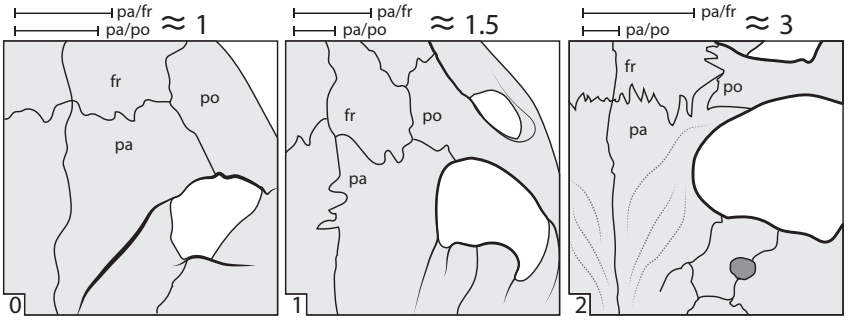

Fig. 8. Illustration of the different states of character 23, on the degree of upper temporal emargination seen as the parietal–postorbital suture length compared to the length of the parietal–frontal contact: 0, broad contact; 1, reduced contact; 2, narrow contact. Abbreviations: f.n., fossa nasalis; mx, maxilla; pm, premaxilla.

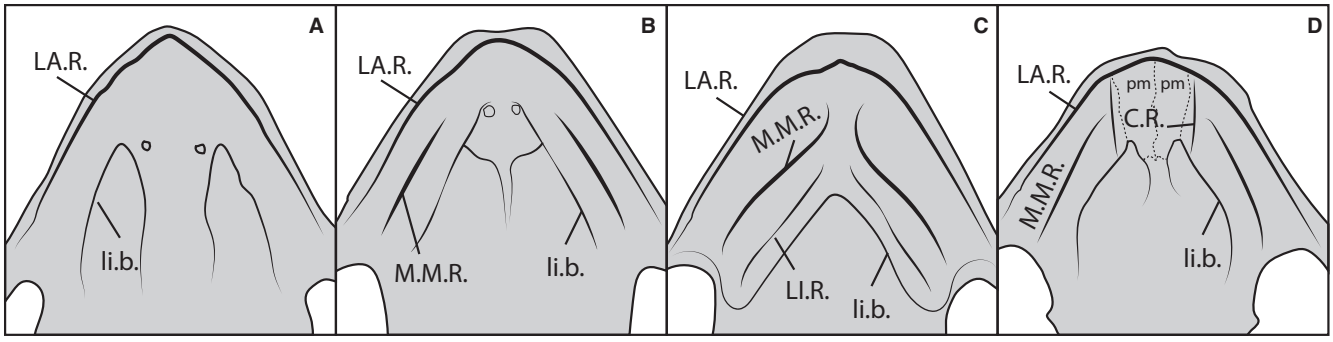

Fig. 9. Illustration of the different states of characters 29–31: A, no ridges present in the triturating surface (*Kinixys homeana*); B, median maxillary ridge present (*Chrysemys picta*); C, both median maxillary ridge and lingual ridge present (*Batagur baska*); D, commissural ridge present (*Chelonoidis chilensis*). Abbreviations: C.R., commissural ridge; LA.R, labial ridge; li.b., lingual border; LI.R., lingual ridge; M.M.R., median maxillary ridge; pm, premaxilla.

characters regarding the ridges in the triturating surfaces is difficult and not consistent in the literature. As Gaffney (1979:89) notes, a "labial ridge" refers to the most lateral ridge, whereas a "lingual ridge" refers to the most medial one. However, as Gaffney (1979: 89) correctly points out, these terms are merely positional and do not imply homology. The definition of the (most lateral) labial ridge (LA.R.) is clear and most probably homologous between the various taxa, but the homology of the lingual ridge (LI.R.) is less straightforward. Some authors consider the lingual border of the maxilla (li.b.) and the lingual ridge to be identical (e.g., Luján et al., 2014). Even if the lingual border of the maxilla appears rounded and protruding (usually medially) as a ridge, here we do not consider it as a lingual ridge in the strict sense. Instead, we propose to use the complex morphology seen in *Batagur baska* as a reference to define ridges in the triturating surface. The ridge found in *Ba. baska* just lateral to the lingual border of the maxilla is termed here as the lingual ridge (LI.R.), and the lateral margin of the maxilla is termed the labial ridge (LA.R.). Between and roughly parallel to the LI.R. and the LA.R., an extra ridge is developed, termed here as the median maxillary ridge (M.M.R.; as in TA). Consequently, *Kinixys homeana* is scored as having no L.I.R. and no M.M.R. and *Chrysemys picta* as having only an M.M.R., whereas *Ba. baska* is scored as having both present. We choose to define discrete binary characters for each ridge because they are independent structures and to account for the double transformation cost of having all three ridges (as in *baska*). Our scoring of the taxa is probably roughly similar to that of JB, but the definition is different.

In other cases, a ridge is formed parallel or coinciding with the maxilla/premaxilla suture (e.g., in *Chel. chilensis*). This is termed as a commissural ridge [C.R.; as in McDowell 1964, CT18; transverse (= commissural) ridge in MS11)].

32, Median ridge or sulcus of the triturating surface of the upper jaw:

0 = both structures absent; 1 = median ridge present; 2 = median sulcus present | **JB32**; MS10

33, Lingual border of upper triturating surface joining in premaxillae and forming a well-developed ridge (e.g., *Gopherus* spp.)

0 = absent; 1 = present | MS13, GE13

Definition: Following the previous definition of the lingual ridge, the definition of this character is modified from MS13 and GE13. In some cases (e.g., *Gopherus* spp.), the lingual border of each maxillae extends anteriorly to meet in the premaxillary symphysis.

34, Extent of the median maxillary ridge in the premaxillae:

0 = restricted to the maxilla; 1 = extending to the premaxillae | **MS12** (modified)

Definition: In some cases, the median maxillary ridge could extend to the premaxillae. This character can be clearly observed in the extant *M. impressa* and the extinct *He. crassiscuttata* and *He. bermudae*. In some cases, (e.g., *M. impressa* and *He. crassiscutata*) they could meet in the midline or in *He. bermudae*, they terminate in the commissural ridge.

Based on the available sample, the development of the commissural ridge could result in the separation of the median maxillary ridge in the midline and therefore a state "median maxillary ridge extending to the premaxillae but not meeting in the midline" seems redundant.

35, Tooth-like tubercles on the labial ridge:

0 = absent; 1 = present | GE17, CT13 (modified)

Definition: Character GE17 was simply coding the presence of fine, tooth-like tubercles (= serrations) in the maxillary ridges. Here, we divided this character per type of ridge as we have noted that the presence of such tubercles is independent in each ridge. The presence of such tubercles should be noted on the bony surface and not on the horny beak.

36, Tooth-like tubercles on the median maxillary ridge:

0 = absent; 1 = present | GE17, CT13 (modified)

See previous character. Tubercles = fine serrations. This character is scored as N/A in taxa with the median maxillary ridge absent.

37, Posterior maxillary process (Fig. 10):

0 = absent; 1 = present | **CR-PMP**; MS15; CT12

38, Vomerine foramen:

0 = absent; 1 = present | **JB19**

39, Posterior extension of the vomer reaching the basisphenoid (Fig. 11):

0 = vomer short, not dividing the palatines; 1 = vomer dividing the palatines, may touch or may not touch the pterygoids; 2 = vomer dividing part of the pterygoids, not reaching the basisphenoid; 3 = vomer dividing palatines and pterygoids, reaching the basisphenoid | MS17; **GE24**

40, Posterior extension of the vomer ridge:

0 = vomer ridge present in the anterior 2/3 of the vomer; 1 = vomer ridge present also on the posterior third | GE21 (part)

41, Vomer ridge "flag":

0 = absent; 1 = present | GE21

42, Vomer shape:

0 = flat anterior portion of vomer, and roughly parallel sides, no ridge; 1 = fan-shaped anterior part of the vomer, usually the ridge (see above) extends to this point | GE20 (part)

43, Development of the foramen praepalatinum as a canal (canalis praepalatinum) that is concealed by a bony secondary palate in ventral view:

0 = absent; 1 = present | MS14 (part); GE27 + 28; **JB20**

44, Foramen carotico-pharyngeale:

0 = present, large; 1 = reduced; 2 = absent | CT4

ORDERED

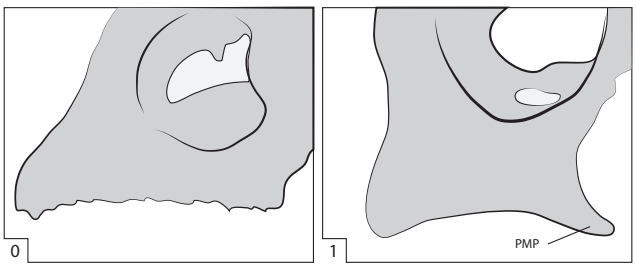

Fig. 10. Illustration of the different states of character 37: 0, posterior maxillary process absent in *Stigmochelys pardalis*; 1, present in *Gopherus polyphemus*. Abbreviations: PMP, posterior maxillary process.

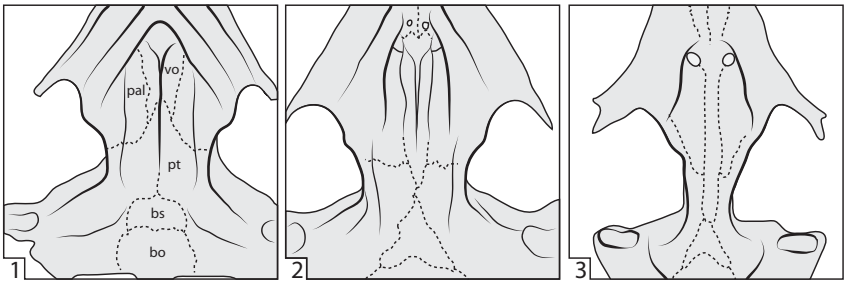

Fig. 11. Illustration of the different states of character 39, on the length of the vomer (state 0 not figured): 1, vomer dividing the palatines, not the pterygoids in *Gopherus polyphemus*; 2, vomer diving part of the pterygoids, not reaching the basisphenoid in *Centrochelys sulcata*; 3, vomer dividing palatines and pterygoids, reaching the basisphenoid in *Geochelone elegans*.

Definition: We define state 0 as the condition seen in *Kinosternon odoratus*, where the foramen is clearly visible and much larger than the condition seen in most emydids, geoemydids and some testudinids (our state 1). In most testudinids this foramen is absent on the ventral side of the pterygoid. Based on this definition, this character could be ordered.

45, Contact between pterygoid and basioccipital:

0 = present; 1 = absent | CR-BR; **JB21**; CT2

Definition: CT1 defined a character for the width of the contact between the basioccipital and the basisphenoid (narrower in Emydidae). Although they acknowledge that CT1 and CT2 are correlated to some extent, they found some difference in the molluscivorous emydid species. We have been unable to score with confidence the states of the CT1 character (which should be coded in a continuous fashion). Thus, CT1 is not included here. Our data on *Chelonoidis carbonaria* and *Chelonoidis denticulata* confirm the observations of JB21 for a strong ontogenetic component in this character.

46, Contact of the pterygoid with the articular facet of the quadrate:

0 = absent; 1 = present | JB22

47, Position of the processus pterygoideus externus (p.p.e.) relative to the foramen palatinus posterious (f.p.p.):

0 = p.p.e. is situated clearly posterior to f.p.p.; 1 = p.p.e. is situated at the same level with the f.p.p.; 2 = p.p.e. is situated clearly anterior to f.p.p |

48, Closure and depth of the incisura columella auris:

0 = absent, incisura is open; 1 = present, incisura closed | CR-SEQ; GM-H1.3; GE35; **JB23**; CT8

49, Processus interfenestralis:

0 = visible in ventral view; 1 = not visible in ventral view | **GE36**

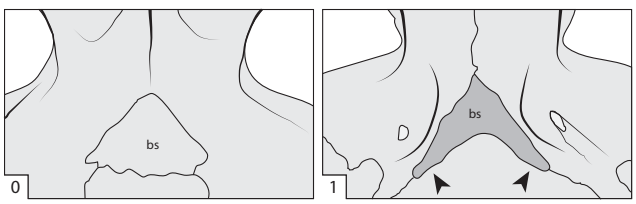

Fig. 12. Illustration of the states of character 50, basisphenoid (bs) shape: 0, not V-shaped; 1, V-shaped.

50, Basisphenoid shape (Fig. 12):

0 = not V-shaped; 1 = V-shaped (postero-lateral processes present)

Definition: Normally, the basisphenoid is triangular in shape. In some tortoises, the basisphenoid bone is V-shaped, sending two postero-lateral processes.

51, Degree of expansion of the opisthotic in posterior view:

0 = not expanded, fenestra postotica open, contacts exoccipital; 1 = expanded, contacts basioccipital but not the pterygoid; 2 = expanded, contacting the pterygoid | **GE50** (modified)

ORDERED

Definition: This character is based on GE50, which was created on the visibility of the fenestra postotica in posterior view based mainly on the degree of the expansion of the opisthotic. We have been unable to clearly observe the various states of GE50, especially those that refer to the kind of ossification. We have modified this character referring to the contacts of the opisthotic with the surrounding elements and to form a morphocline.

52, Position of the foramen jugulare posterius:

0 = located in the exoccipital bone; 1 = located in the exoccipital/opisthotic suture |

53, Extent of the squamosals:

0 = extending beyond the condylus occipitalis; 1 = not extending beyond the condylus occipitalis | **GE38**

54, Horizontal keels in crista supraoccipitalis:

0 = absent; 1 = present | **GE43**

55, Shape of crista supraoccipitalis (Fig. 13):

0 = bended downwards; 1 = straight; 2 = elevated posteriorly | **PV30**

56, Length of crista supraoccipitalis:

0 = extending more than twice the length of the neck of condylus occipitalis (measured from the neck); 1 = extending less than twice the length | HI40 (modified); GE42

Definition: Length is measured in ventral view on the portion extending beyond the occipital condyle. The neck of the occipital condyle involves the proximal limit of the neck but excludes the condyle. The character is intended to capture the taxa with a notably long crista supraocipitalis.

57, Processus trochlearis oticum:

0 = absent or small; 1 = large | CR-TP; **GE54**

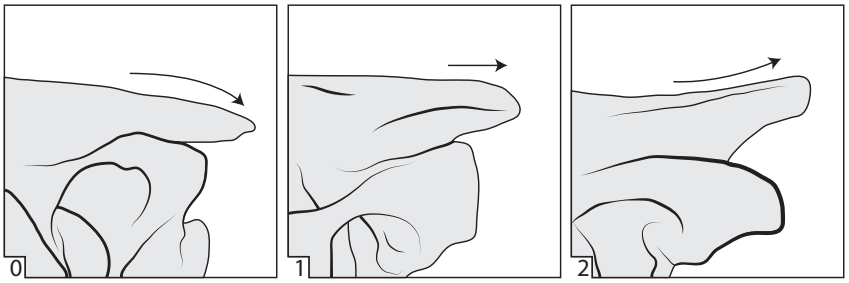

Fig. 13. Illustration of the different states of shape of crista supraoccipitalis: 0, bent downwards in *Gopherus polyphemus*; 1, straight in *Centrochelys sulcata*; 2, elevated posteriorly in *Kinixys erosa*.

Mandible characters

58, Angular contribution to the sulcus cartilaginis Meckelii:

0 = present, the angular contributes to the sulcus and is as long as or longer than the prearticular; 1 = absent, the angular is shorter than the prearticular | CR-AMG; **JB24**; CT6

59, Contact between surangular and dentary:

0 = simple contact; 1 = strongly interdigitated suture | CR-SP; GM-H6.1; GE62; MS21; **JB25**

60, Height of the processus coronoideus:

0 = as high as dentary; 1 = higher than the dentary; 2 = rising significantly above the dentary | **JB26** (modified) ORDERED

Definition: We have added an intermediate state to JB26 and ordered the character.

61, Foramen dentofaciale majus:

0 = small; 1 = large and situated within a large lateral fossa | **JB27**

62, Foramen nervi auriculotemporalis:

0 = absent; 1 = present

63, Foramen nervi auriculotemporalis shape:

0 = large; 1 = small

64, Foramen alveolare inferius & foramen intermandibularis medius:

0 = separated; 1 = fused

65, Foramen alveolare inferius:

0 = coronoid involved; 1 = coronoid excluded

66, Foramen intermandibularis caudalis:

0 = absent or very small; 1 = present

67, Prearticular bone:

0 = not extending beyond the coronoid in lingual view; 1 = extending beyond the coronoid

68, Foramen intermandibularis oralis:

0 = present; 1 = absent

69, Angle of the dentary symphysis:

0 = <60°; 1 = >60° | **GE60**

70, Posterior extension of the lower triturating surface behind the symphysis of the dentary:

0 = absent; 1 = present | **JB33**

71, Presence of dentary hook:

0 = absent; 1 = present

72, Shape of dentary hook:

0 = smooth; 1 = medial tooth present

Definition: In some taxa (e.g., *Batagur baska*), the dentary hook terminates in a single, basally constricted, tooth-like process. Scored as N/A in taxa without a dentary hook.

73, Presence of dentary serration:

0 = absent; 1 = present

74, Dentary serration:

0 = present in labial ridge; 1 = present in both lingual and labial ridges

Definition: Scored as N/A in taxa without dentary serration.

75, Well-developed serrations on labial or lingual ridges of the triturating surfaces of the upper and lower jaws:

0 = absent; 1 = present | **JB32**

Cranial characters

76, Carapace strongly tricarinate in adult:

0 = absent; 1 = present | **JB34**; CT32

77, Carapace of adult tectiform in cross-section with a strong posterior projection on the third vertebral scute:

0 = absent; 1 = present | **JB36**

78, Postero-lateral side of nuchal (Fig. 14):

0 = straight; 1 = anteriorly concave

79, General shape of the nuchal (Fig. 15):

0 = markedly wider than long; 1 = about 1/3 wider than long or as long as wide; 2 = markedly longer than wide | HE22; **PV2** ORDERED

80, Overlapping of the first pleural on the nuchal plate (Fig. 16):

0 = first pleural overlaps the postero-lateral corner of the nuchal; 1 = first pleural touches, but it does not overlap the nuchal; 2 = first pleural is not in contact with the nuchal | ORDERED

81, Posterior margin of first vertebral scute significantly narrower than its anterior margin:
0 = absent; 1 = present | **JB44**

82, Anterior half of the first vertebral scute much narrower than posterior half, especially in adults:
0 = absent; 1 = present | **JB45**

83, Nuchal notch:
0 = absent; 1 = present | HE4; **PV1** (modified)

84, Anterior protrusion of the nuchal:
0 = absent; 1 = present

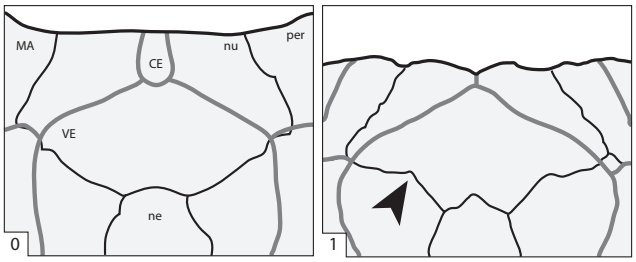

Fig. 14. Illustration of the different states of character 78, on the postero-lateral side of nuchal: 0, straight in *Testudo graeca*; 1, anteriorly concave in *Geochelone elegans*.

85, Number of neural plates:
0 = nine; 1 = eight; 2 = seven or less | **CT27**; FLB5; PV3

86, Shape of the first neural:
0 = hexagonal, short sides positioned posteriorly; 1 = rectangular | CT28 (modified); **PV6**

87, Shape and orientation of the second neural:
0 = second neural hexagonal, short sides positioned anteriorly; 1 = second neural hexagonal, short sides positioned posteriorly; 2 = rectangular; 3 = second neural octagonal | **JB37** (modified); CT28 (modified); PV7
Definition: A state representing a rectangular second neural (as in *Ach. cassouleti*) is added. The scoring is similar as in JB37.

88, Shape and orientation of the third neural:
0 = third neural hexagonal, short sides positioned anteriorly; 1 = third neural hexagonal, short sides positioned posteriorly; 2 = third neural square; 3 = third neural octagonal | **JB38**; CT28 (modified); PV8

89, Shape and orientation of the fourth neural:
0 = fourth neural rectangular; 1 = fourth neural hexagonal; 2 = fourth neural octagonal | **PV9**

90, Shape of the fifth neural:
0 = hexagonal; 1 = rectangular | CT28 (modified); **PV10**

91, Number of suprapygals:
0 = two; 1 = one | CR-PYP; FLB6-7; **PV11**

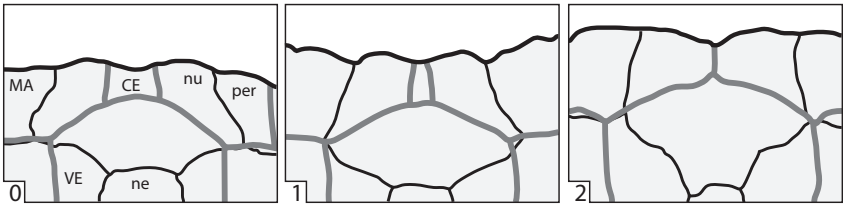

Fig. 15. Illustration of the different states of character 79, on the shape of the nuchal: 0, markedly wider than long in *Gopherus agassizi*; 1, as wide as long in *Testudo graeca*; 2, longer than wide in *Centrochelys sulcata*. Abbreviations: CE, cervical; MA, marginal; ne, neural; nu, nuchal; per, peripheral; VE, vertebral.

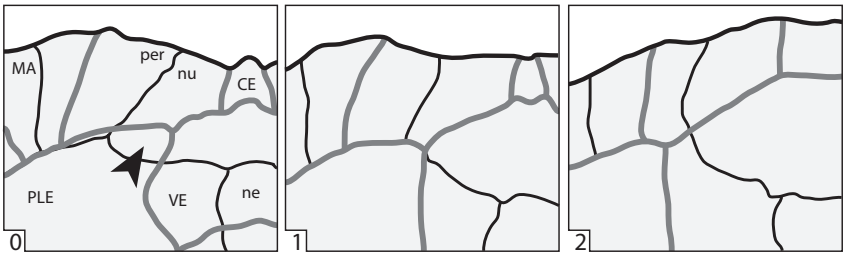

Fig. 16. Illustration of the different states of character 80, on the overlapping of the first pleural on the nuchal plate: 0, first pleural overlapping the nuchal in *Testudo kleinmanni*; 1, first pleural touches, but it does not overlap the nuchal in *Testudo graeca*; 2, first pleural is not in contact with the nuchal in *Gopherus polyphemus*. Abbreviations: CE, cervical; MA, marginal; ne, neural; nu, nuchal; per, peripheral; PLE, pleural; VE, vertebral.

92, Shape of the suprapygal bones (Fig. 17):

0 = two, the contact between the suprapygals is straight and perpendicular to the axial plane; 1 = two, first suprapygal embraces the lenticular second one; 2 = one, suprapygals fused, constituting one trapeze | CR-PYP; FLB6-7; **PV11**

93, Shape of costal rib head:

0 = flat and wide; 1 = thin and elongated

94, Width of the costovertebral tunnel (medially) (Fig. 18):

0 = Wide; 1 = Medium; 2 = Narrow | ORDERED

Definition: These two characters have been observed in neurals 3 to 6. For defining character 94, we use the ratio between the width of the neural and the width between the entering points of the ribs (see figure below). State 0 could be defined as having values close to 2.0, state 1 as between 1.7 and 1.2 and state 2 close to 1.0. These ranges have been calculated based on our sample, but note that perhaps this character should be analysed as a continuous one in the future. Since state 1 is a true intermediate state, the character is ordered. In the outgroup (*Chelydra serpentina*), the shape of costal rib head (characher 93) is flat and wide and forms a large costovertebral tunnel (0;0). Emydids show costal rib heads that are flat and located far from the neural/costal suture (0;1), whereas the width of the costovertebral tunnel in geoemydids is even narrower (0;2). The testudinids on the other hand show much thinner and elongated rib heads, almost needle-like, which are exiting the costal at the suture with the neural in most cases (1;2).

95, Medial contact of the seventh and/or eighth costal bones:

0 = absent; 1 = present | **JB39**

96, Pygal shape:

0 = quadrangular; 1 = hexagonal with small antero-lateral borders | **FLB8**

97, Pygal notch:

0 = absent; 1 = present

98, Coincidence between the costo-peripheral suture and the pleuromarginal sulcus (exc. nuchal and pygal area):

0 = absent; 1 = present | HE16; FLB4; **PV15**

99, Significant serration of the posterior peripherals:

0 = absent; 1 = present | **JB35**

100, Protrusions of the peripherals on the limit with the sulci between the marginals:

0 = absent or poorly developed; 1 = well developed | **PV12 + PV13**

101, Cervical scute:

0 = present; 1 = absent | CR-CVS; JB40; CT33; FLB13; PV14

102, Shape of the cervical scute:

0 = longer than wide; 1 = wider than long | **MS1**(modified)

Comment: Scored as N/A in those lacking the cervical scute.

103, Length of the cervical scute in dorsal view:

0 = short, equal or less than 25% of the nuchal length; 1 = long, longer than 25% of the nuchal length | **HE12** (modified)

Comment: Scored as N/A in those lacking a cervical scute.

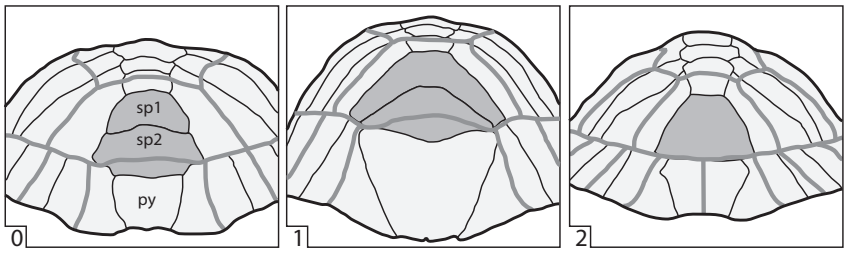

Fig. 17. Illustration of the different states of character 92, on the shape of the suprapygal bones: 0, two suprapygals with straight contact in *Gopherus polyphemus*; 1, two suprapygals, the first embracing the second, in *Stigmochelys pardalis*; 2, one suprapygal in "*Testudo*" *hermanni*. Abbreviations: py, pygal; sp, suprapygal.

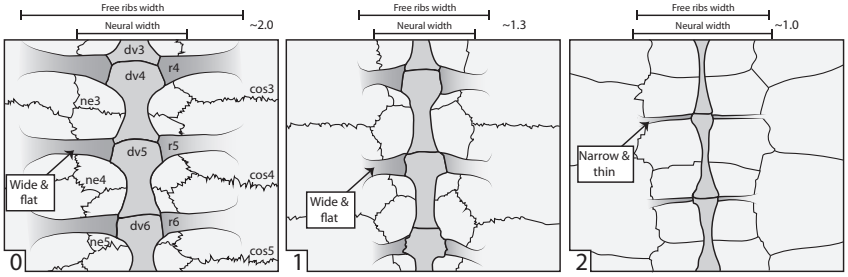

Fig. 18. Illustration of character 94, on the width of the costovertebral tunnel: 0 = wide in Chelydra serpentina; 1 = medium in Chrysemys picta; 2 = narrow in Chelonoidis carbonaria. Abbreviations: cos, costal; dv, dorsal vertebra; ne, neural; r, rib. Also the states of the previous character are illustrated.

104, Number of vertebral scutes:
0 = five; 1 = six or more | **JB41**

105, Width of the vertebrals relative to pleurals:
0 = wide vertebrals, wider than the pleurals; 1 = wide vertebrals, almost equal to the pleurals; 2 = narrow vertebrals, narrower than the pleurals | HE10; **CT30** (modified) ORDERED

106, Position of the anterior sulcus of the fourth vertebral scute:
0 = sulcus lies on the fifth neural; 1 = sulcus lies on fourth neural, or on the suture between the fourth and fifth neural; 2 = sulcus lies on the sixth neural, or on the suture between the fifth and sixth neural | **JB42**

107, Position of the posterior sulcus of the fourth vertebral scute:
0 = sulcus lies on the eighth neural, or on the homologue of the eighth neural, if the seventh is reduced (e.g., in most tortoises); 1 = sulcus lies on the seventh neural or on the suture between the seventh and eight neural; 2 = eighth neural absent, sulcus overlies costals that meet at the midline | **JB43**

108, Contact of the second marginals with the lateral margin of the nuchal:
0 = absent; 1 = present | **PV16**

109, Contact of the second marginal scute with the first vertebral scute:
0 = absent; 1 = present | **JB47**; PV17

110, Contact of the sixth marginal scute with the third pleural scute:
0 = absent; 1 = present | CR-MP; HE19; **JB48**; CT25; PV18

111, Significant contact of the tenth marginal scute with the fifth vertebral scute:
0 = absent; 1 = present | HE20; **JB46**

112, Overlapping of fifth vertebral on suprapygal (Fig. 19):
0 = the posterior sulcus of the fifth vertebral overlaps the anterior part of the pygal; 1 = the posterior sulcus of the fifth vertebral coincides with the suprapygal-pygal suture; 2 = the posterior sulcus of the fifth vertebral crosses the suprapygal transversely | **HE21** (modified) ORDERED

113, Twelfth marginal scutes in dorsal view:
0 = divided; 1 = fused | MS4; JB49 (modified); CT24; FLB15 + 16; **PV19**
Comment: We have modified the character of JB49, as it originally referred to two different morphologies, the fusion of the twelfth marginals and the extension of the fifth vertebral on the suprapygal (see previous character). Here we retain only two states.

114, Carapacial hinge:
0 = absent; 1 = hinge present, as in *Kinixys* | **CR-CRH**

115, Shape of the posterior carapace border:
0 = curved inwards; 1 = posterior border posteriorly flared | **FLB2** (part)

116, Sutured contact between plastron and carapace:
0 = present, plastron and carapace are tightly connected by an osseous bridge; 1 = absent, plastron is attached to carapace by connective tissue | **JB50**

117, Presence and development of anterior buttresses:
0 = anterior buttresses absent; 1 = anterior buttresses present but small, and not in contact with the first costal bones; 2 = anterior buttresses long and thin and just barely in contact with the costal bones, if at all; 3 = anterior buttresses well developed and in clear contact with the first costal bones; 4 = anterior buttresses very large and in direct contact with the first dorsal rib | **JB51** ORDERED

118, Presence and development of posterior buttresses:
0 = posterior buttresses absent; 1 = posterior buttresses present but small, and not in contact with the costal bones; 2 = posterior buttresses long and thin and just barely in contact with the costal bones, if at all; 3 = posterior buttresses well developed and in clear contact with costal bones V and VI; 4 = posterior buttresses well developed but only in clear contact with costal bone V | **JB52**; CT34 ORDERED
Comment: these two characters of JB51-52 have been ordered as the various states are generally continuous.

Plastron characters

119, Shape of the anterior lobe:
0 = subrounded to straight; 1 = medially notched; 2 = trilobed | HE37; **PV21**

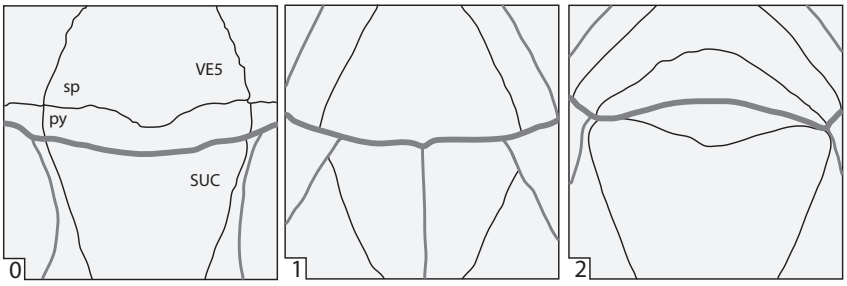

Fig. 19. Illustration of the different states of character 112, on the overlapping of fifth vertebral on suprapygal: 0, vertebral 5 overlapping the anterior pygal in *Kinixys erosa*; 1, vertebral 5 crossing the suprapygal transversely in *Stigmochelys pardalis*; 2, coinciding with the suprapygal-pygal suture in "*Testudo*" *hermanni*. Abbreviations: py, pygal; sp, suprapygal; SUC, supracaudal; VE, vertebral.

120, Well-developed gular protrusion, caused by constriction in the gularo-humeral sulcus:
0 = absent; 1 = present | CR-PLC (part); **PV22**

121, Extensive overhanging lip of the epiplastra:
0 = absent; 1 = present | MS5; **JB59**; FLB9&10 (part)

122, Shape of the dorsal lip of the epiplastra:
0 = concave; 1 = relatively flat; 2 = clearly convex | **PV23** (modified); FLB9 (part) ORDERED
Definition: This character is scored as N/A in those lacking an epiplastral lip. As the three states are more or less continuous, this character is analysed as ordered, to account for the greater transformation cost from state 0 to state 2.

123, Contact between the gulars and the entoplastron:
0 = not in contact; 1 = in contact with the anterior margin; 2 = covering the anterior area of entoplastron | CR-GSE (part); MS6 (part); HE32; **PV24** ORDERED
Comment: As the three states are continuous and state 1 is a true intermediate, this character is ordered.

124, Angle formed by gularo-humeral sulcus:
0 = >90°; 1 = 90–60°; 2 = <60° | **PV28** (modified)
ORDERED
Comment: As the three states are continuous and state 1 is a true intermediate, this character is ordered.

125, Median anteroposterior length of humerals, compared to the median length of gulars:
0 = humerals equal to or shorter than gulars; 1 = humerals longer than gulars

126, Shape of the humero-pectoral sulcus medially:
0 = not perpendicular to the axial plane, rounded or forming a wide angle; 1 = perpendicular to the axial plane; 2 = wavy, i.e., medially convex, laterally concave | MS7 (part); CR-PEC (part); **PV25** (modified)

127, Shape of the lateral portion of the humero-pectoral sulcus
0 = perpendicular to the axial plane, relatively straight throughout its width; 1 = perpendicular to the axial plane and concave 2 = perpendicular to the axial plane and convex |
Comment: Scored as N/A in taxa having state 0 or 2 for character 126 (see above).

128, Position of the humero-pectoral sulcus relative to the entoplastron:
0 = posterior to the entoplastron; 1 = coinciding medially with the posterior contact of the entoplastron-hyoplastron; 2 = crossing the entoplastron | **JB60** (modified) ORDERED
Comment: We have added an intermediate state for the condition seen in several taxa.

129, Medial length of pectorals:
0 = long; 1 = short | **PV26**
Definition: Testudinids show short pectoral scutes medially compared to other testudinoids.

130, Medially directed pivoting process for plastral hinge developed on fifth peripheral bone:
0 = absent; 1 = present | **JB53**

131, Plastral hinge:
0 = absent; 1 = present, between hyoplastra and hypoplastra; 2 = present, between hypoplastra and xiphiplastra | CR-APH; CR-PPH; JB54; FLB3; FLB11(part); PV27

132, Contact between inguinal and femoral scutes:
0 = absent; 1 = present | CR-ING (part); MS9; **JB55**

133, Presence of axillary glands:
0 = present; 1 = absent | GM-H1.4; **JB56** (modified)

134, Presence of inguinal glands:
0 = present; 1 = absent | GM-H1.4; **JB56** (modified)
Definition: The original character JB56 has been divided into a simple present/absent character, in order to present different groupings between taxa regarding which glands they lack. The problem of the original character states is that they do not allow scoring a taxon that has only inguinal glands (if any). The final scoring follows JB 56. See also next two characters on musk duct foramina.
Example: *Emys orbicularis* shows only axillary glands but *barbouri* has lost both (JB56 and references therein). Based on the original scoring of JB56, *Gra. barbouri* (scored as 2; musk glands absent) and *Em. orbicularis* (scored as 1; axillary glands present only) could never be grouped based on the scoring of this character, although they are more similar to each other in the absence of inguinal glands compared to turtles that retain the inguinal glands. With the new scoring (*barbouri* as 1;1 and *orbicularis* 0;1) they differ in the presence of axillary glands but they could be grouped by the absence of inguinal glands.

135, Presence of anterior musk duct foramina:
0 = present; 1 = absent | GM-H1.4; MS8; **JB57** (modified); CT36

136, Presence of posterior musk duct foramina:
0 = present; 1 = absent | GM-H1.4; MS8; **JB58** (modified); CT36
Definition: Given the definition of the gland character (see above), the original characters JB57 and JB58 have been simplified to describe only the musk duct foramina, to avoid repetition in the scoring of musk glands. With the new scoring, taxa with the musk duct foramina absent (previously scored as 1 and 2) are scored as 1 and they can be grouped together. Taxa that lack musk glands (and thus cannot have any musk duct foramina) are scored as N/A.

137, Shape of the femoro-anal sulcus:
0 = forms an acute angle with the axial plane; 1 = straight or slightly rounded, developed mainly perpendicular to the axial plane; 2 = omega-shaped

138, Medial length of the anals:
0 = shorter than the median length of femoral; 1 = longer than the medial length of femoral

139, Anal notch of the plastron:
0 = present; 1 = absent | **JB61** (modified)

140, Anal notch shape 1:
0 = deep; 1 = reduced

141, Anal notch shape 2:
0 = angular; 1 = rounded
Definition: We divided the original character of JB61 in three. The first character (presence/absence of anal notch) provides a grouping of taxa with an anal notch, whereas the remaining two characters provide groupings based on the shape. Taxa without an anal notch are scored as N/A for characters 141 and 142.

142, Anal scutes fused:
0 = absent; 1 = present | **JB62**

143, Plastral scutes with vibrant, radiating colour pattern:
0 = absent; 1 = present | **JB63**

Appendicular characters

144, Position of biconvex cervical vertebra:
0 = fourth vertebra; 1 = third vertebra | **CR-PBV**; GM-H2.6
Definition: Our scoring largely follows CR-PBV, as we have been able to confirm most of his scorings. Additional information is taken from Williams (1950) and personal observations.

145, Shape of cervical vertebra 2:
0 = longer than tall; 1 = short & tall

146, Dorsal process on cervical vertebra 3:
0 = present; 1 = absent

147, Postzygapophyses sloping anteriorly on cervical vertebra 5:
0 = present; 1 = absent

148, Ventral keel on cervical vertebra 7:
0 = anteriorly placed; 1 = rounded and symmetric ventral outline; 2 = low

149, Dorsal process on cervical vertebra 8:
0 = prominent; 1 = not prominent | **CR-DVC**

150, Ventral keel on cervical vertebra 8:
0 = all along the centrum; 1 = isolated in the middle

151, Shape of coracoid blade:
0 = long and narrow; 1 = short and very wide | MS23; **JB66**

152, Latissimus dorsi scar:
0 = absent or reduced; 1 = present | CR-LDS; **MS26**

153, Major trochanter of the humerus, in relation with the humeral head:
0 = short, not extending beyond the humeral head; 1 = long, extending beyond the humeral head | **MS25**

154, Ventral ischial tubercle in pelvis:
0 = not triagonal; 1 = triagonal in ventral view

155, Angle between the femoral head and the diaphysis of the femur:
0 = relatively large; 1 = femoral head developed almost perpendicular to the diaphysis | **PV36**

156, Trochanters of the femur:
0 = not fused; 1 = fused | MS27; **FLB17**

157, Contact between radius and distal carpals:
0 = length of centralia extensive, preventing the contact of radius and distal carpals; 1 = length of centralia reduced, contact between radius and distal carpals present | **CR-MEC**; GM-H6.3
Comment: The scorings are based on both personal observations, as well as the detailed figures from Crumly (1984). On fossil taxa this character has been scored in *Ti. bacharidisi*, *Ti. bolivari* and *Sty. nebraskensis*. Although probably the condition in *Ti. perpiniana* is similar to *Ti. bacharidisi*, the state of preservation does not allow a confident assessment.

158, Fusion of medial and lateral centrale:
0 = not fused; 1 = fused | **CR-CNF**

159, Fusion of calcaneus and astragalus:
0 = not fused; 1 = fused | **CR-CA**

160, Number of manual claws:
0 = five; 1 = four | **JB67**

161, Webbing between digits:
0 = present, well developed; 1 = absent, or at least strongly reduced | **JB69**

162, Digit 1 phalangeal number manus:
0 = two; 1 = one; 2 = zero | Based on Crumly & Sánchez-Villagra (2004). Similar in: CR-PHN; JB68 (modified)

163, Digit 2 phalangeal number manus:
0 = two; 1 = one; 2 = zero

164, Digit 4 phalangeal number manus:
0 = two; 1 = one; 2 = zero

165, Digit 5 phalangeal number manus:
0 = two; 1 = one; 2 = zero
Comment: Compared to numerous other works that code each taxon with a phalangeal formula (i.e., 2-3-3-3-2), we code each digit separately based on the number of phalanges present (note: without counting the manual claw). Definition and scoring follows Crumly & Sánchez-Villagra (2004) .

166, Fifth phalanx in the pes:
0 = present, visible externally; 1 = not visible externally, vestigial present internally; 2 = completely absent | **CR-FPA** (modified) ORDERED
Comment: Most of the observations of CR-FPA have been confirmed in our, much smaller, sampling. The scoring of CR-FPA is therefore largely followed here. A third state (0) has been added for the outgroup and the character is analysed as an ordered one.

167, Dermal armour (osteoderms) on limbs:
0 = absent; 1 = present | **MS28** (part)

168, Type of dermal armour:
0 = thigh spurs; 1 = thigh plate; 2 = caudal buckler | **CR-CB** (partial)
Comment: Scored as N/A in those not having a dermal armor.

Miscellaneous characters

169, Development of a suprascapula:
0 = absent; 1 = present | **JB64**

170, Development of an episcapula:
0 = absent; 1 = present | **JB65**

171, Sexual size dimorphism:
0 = absent; 1 = present, maximum body size of female much larger than male | **JB70**

Characters omitted: Below, we list some characters from the abovementioned works that are tentatively omitted from our analysis for various reasons. Mainly, some characters are either non-informative for the analysed taxa, others show an unclear definition that has resulted in our inability to replicate the scorings, and others require more sampling to test the potential validity of these characters.

Non-informative/redundant with other characters. **Crumly, 1984;** : ENO, INO; **Gerlach, 2001**: 20, 39, 41, 48, 55; **Claude and Tong, 2004**: 10, 17, 26, 29, 31; **Pérez-García and Vlachos, 2014**: 29, 31, 32, 34, 35.

Unclear definition/inability to replicate the scorings. **Crumly, 1984;**: BRT, BTP, EPC, MAN, MAX, PF, ITF, MPB, ALT; **Gerlach, 2001**: 5, 6, 18, 23, 30, 32, 34, 37, 40, 47, 49, 55, 59; **Lapparent de Broin et al., 2006**: 0, 1, 12.

Potentially valid, more sampling is needed. **Crumly, 1984**: FCL, MEC, PSF, FUI, CRF; **Gerlach, 2001**: 33, 51, 52, 53, 56, 57;.

Information on the specimens and papers examined for scoring of the characters on the analysed taxa.

Note: The scorings of the taxa from Joyce and Bell (2004) have been checked and confirmed and the only changes in their matrix refer to some modifications on the character definitions (see above).

Institutional Abbreviations: **AMNH**, American Museum of Natural History; **AMPG**, Museum of Palaeontology and Geology of the National and Kapodistrian University of Athens, Greece; **BSPG**, Bayerische Staatssammlung für Paläontologie und Geologie, Munich, Germany; **CRI**, Chelonian Research Institute (P. Pritchard), USA; **LGPUT**, Laboratory of Geology and Paleontology of University of Thessaloniki; **MCNUS**, Museum of Salamanca, Spain; **MPEF**, Museo Paleontológico Egidio Feruglio, Trelew, Chubut, Argentina; **NHMW**, Naturhistorisches Museum, Vienna, Austria; **MNCN**, Museo National de Ciencias Naturales, Madrid, Spain; **MNHN**, Muséum National d"Histoire Naturelle, Paris, France; **NWS**, Naturmuseum Winterthur, Switzerland; **PIMUZ**, Paläontologische Institut und Museum, University Zurich, Switzerland; **REP**, Comparative Anatomy Collection, MNHN, Paris; SMF, Senckenberg Forschungsinstitut und Naturmuseum Senckenberganlage, Frankfurt Germany; **SMNS**, Staatliche Museum für Naturkunde, Stuttgart, Germany; **STUS**, Sala de las Tortugas de la Universidad de Salamanca, Spain; **UCMP**, University of California Museum of Paleontology, USA; **USNM**, Smithsonian Museum of Natural History, U.S.A; **ZIN**, Zoological Museum of the Russian Academy of Sciences, Moscow, Russia.

Extant taxa:

Gopherus agassizii > UCMP 119060, 119066, 222094.

Chelonoidis carbonaria > AMNH 7042, 7043, 62583-62590; UCMP 119049, 119049, 137990) Herpetological collection of Sao Paulo, Brazil, various specimens.

Chelonoidis chilensis > MPEF specimens.

Chelonoidis denticulata > CRI 284, 287, 2489, 6374, 7702; UCMP 138687; USNM 73932; Herpetological collection of Sao Paulo, Brazil, various specimens.

Geochelone elegans > USNM 167557.

Indotestudo elongata > UCMP 119050, 520645; ZIN 6978.

Kinixys erosa > USNM 63483, 109687, 109696.

Indotestudo forstenii > SMF 73267.

Testudo graeca > ZIN 15727, 18242; USNM 76506; SMF 67588; REP 73; LGPUT uncatalogued.

Chersine hermanni > REP 3, 26; USNM 102222; ZIN 29; LGPUT uncatalogued.

Kinixys homeana > USNM 109685.

Agrionemys horsfieldii > Mlynarksi, 1966 & information on digimorph.org for the cranium.

Manouria impressa > UCMP 136588; REP 63.

Testudo kleinmanni > ZIN 9446; information in Delfino et al. (2009).

Testudo marginata > USNM 499029; ZIN 3941; LGPUT uncatalogued.

Chelonoidis nigra > VCCDRS 860-875; MNHN 1883-230.

Stigmochelys pardalis > UCMP 119051.

Gopherus polyphemus > AMNH 73053; USNM 61059, 167526.

Astrochelys radiata > USNM 167657.

Centrochelys sulcata > MNCN 58823; REP 179, 180.

Malacochersus tornieri > USNM 72539; Mautner et al. (2017).

Extinct taxa:

Gigantochersina ammon > Andrews (1906); Holroyd and Parham (2003).

'Testudo' antiqua > Corsini et al. (2014).

Megalochelys atlas > Setiy Abudi (2009).

Titanochelon bacharidisi > LGPUT specimens in Vlachos et al. (2014); see their supplementary information for detailed numbers.

Hesperotestudo bermudae > Meylan and Sterrer (2000).

Titanochelon bolivari > MNCN and STUS material presented in Pérez-García and Vlachos (2014); see their supplementary information for detailed numbers.

'Ergilemys' bruneti > de Broin (1977).

Paleotestudo canetotiana > de Broin (1977); Lapparent de Broin (2000); Pérez-García & Murelaga (2013).

Fontainechelon cassouleti > Claude and Tong (2004); Pérez-García et al. (2016).

'Hadrianus' castrensis > de Broin (1977).

Hadrianus corsoni > AMNH and USNM specimens; Hay (1908).

'Geochelone' costaricensis > Auffenberg (1971).

Hesperotestudo crassiscutata > AMNH and USNM specimens; Hay (1908); Auffenberg (1963).

'Testudo' eocaenica > Hummel (1935); Pérez-García et al. (2016).

Cheirogaster gigas > MNHN.F.BP 2014; Pérez-García, 2016;.
'Chelonoidis' gringorum > AMNH 3366; MPEF specimens.
'Chelonoidis' hesterna > Auffenberg (1971).
Ergilemys insolitus > Gilmore (1931, 1934).
'Testudo' kaiseni > Gilmore (1931).
Oligopherus laticuneus > Hay (1908); Lambe (1913); Gilmore (1916); USNM specimens.
'Testudo' lunellensis > Delfino et al. (2012).
Testudo marmorum > MNHN PIK 3683; AMPG PIK 1970a-g.
Cheirogaster maurini > de Broin (1977).
Namibchersus namaquensis > Lapparent de Broin (2003, 2008).
Stylemys nebrascensis > Hay (1908); Auffenberg (1961, 1964); USNM specimens.
Mesochersus orangeus > Lapparent de Broin (2003, 2008).
Hesperotestudo osborniana > Hay (1908); Auffenberg (1963); USNM specimens.
'Testudo' oughlamensis > Gmira et al. (2013).
Impregnochelys pachytestis > Meylan & Auffenberg (1986).
Titanochelon perpiniana > MNHN 1887-26.
'Testudo' promarginata > NHMW Prottes 57.
'Testudo' sharanensis > Brinkman et al. (2009).
'Testudo' shensiensis > Brinkman et al. (2009).
Anhuichelys siaoshihensis > Tong et al. (2016).
Pelorochelon soriana > Pérez-García et al. (2016).
Titanochelon vitodurana > NWS 13758; PIMUZ A/III 661.

Additional information used to calibrate the total evidence trees. This was necessary especially for some clades that we had only extant representatives included, in order to visually reduce their long ghost lineages. These taxa were not included in our analysis owing to space constraints and/or available information, but can be assigned to those clades with considerable certainty: *Hadrianus majusculus* from the Ypresian of the USA (to push the origin of Pan-Testudinidae prior to the Eocene). *Gopherus brevisternus* and *Gopherus edae* from the Early Miocene of the USA (to reduce the ghost lineage of *Gopherus*). *Hesperotestudo* from the Early Miocene of the USA (to reduce the ghost lineage of *Hesperotestudo*). *Kinixys* sp. from the Early Miocene Songor Hill (to reduce the ghost lineage of *Kinixys*).